

Design of a
Four-channel Bolometer Module
for ASDEX Upgrade and Tore Supra

E.R. Müller, G. Weber,
F. Mast, G. Schramm,
E. Buchelt, C. Andelfinger

IPP 1/224

October 1985



MAX-PLANCK-INSTITUT FÜR PLASMAPHYSIK

8046 GARCHING BEI MÜNCHEN

MAX-PLANCK-INSTITUT FÜR PLASMAPHYSIK
GARCHING BEI MÜNCHEN

Design of a
Four-channel Bolometer Module
for ASDEX Upgrade and Tore Supra

E.R. Müller, G. Weber,
F. Mast, G. Schramm,
E. Buchelt, C. Andelfinger

IPP 1/224

October 1985

*Die nachstehende Arbeit wurde im Rahmen des Vertrages zwischen dem
Max-Planck-Institut für Plasmaphysik und der Europäischen Atomgemeinschaft über die
Zusammenarbeit auf dem Gebiete der Plasmaphysik durchgeführt.*

IPP 1/224

E.R. Müller, G. Weber,
F. Mast, G. Schramm,
E. Buchelt, C. Andelfinger

Design of a Four-channel
Bolometer Module for
ASDEX-Upgrade and Tore
Supra

October 1985

(in english)

Abstract

A new small-sized four-bolometer module for application in high-temperature plasma diagnostics has been designed. The four bolometers and the four reference bolometers shielded against radiation are placed side by side on one kapton foil, the entire arrangement occupying an area of $2.0 \times 3.3 \text{ cm}^2$. The central part of each bolometer consists of a $1.5 \times 4 \text{ mm}^2$ large, 4 to 15 μm thick radiation absorber made of gold, a 7.5 μm thick kapton carrier foil, and a 0.05 μm thick meander-like gold resistor (conduction path width: 30 μm). It offers all the advantages already provided by the well-known ASDEX and JET bolometers, such as very high operating reliability and resistance to nuclear radiation damage. It is optional to enlarge the cooling time constant of the bolometer in a controlled way from a few milliseconds up to several hundreds, thus improving the sensitivity to very weak signals in the low-frequency ($\leq 20 \text{ Hz}$) part of the radiation spectrum, by means of an additional (thin) gold layer that delays the heat losses from the bolometer foil to the cooling body. Since the bolometer is very suitable for AC-bridge electronics and all bridge resistors are arranged on a minimum area interference signals should be suppressed to extremely low levels.

1. Introduction

Bolometric diagnostics is one of the principal diagnostics in present-day large tokamak experiments, such as ASDEX and JET. The bolometers quantitatively measure the spatial distribution of the radiation and neutral particle emission of the plasma with a time resolution in the millisecond range. The electromagnetic line radiation originates from impurities and is mainly located in the vacuum ultraviolet and soft X-ray parts of the spectrum, the neutral particle losses being mainly due to atomic charge exchange processes.

A decade ago, the radial profiles of radiation in the poloidal plasma cross-section were determined by a shot-to-shot scan performed with one bolometer /1/. After development of a new metal resistor bolometer /2/ suitable for series production, a 19-bolometer array installed in ASDEX has provided complete radiation profiles during a single shot with high time resolution /3/. With circular symmetry assumed in the poloidal plane, the radial profiles have been calculated from the measured chord intensities by means of the Abel inversion method. In JET, three bolometer arrays viewing the poloidal plane at different angles reveal details of an actually two-dimensional radiation distribution /4,5/. In future tokamaks, such as ASDEX Upgrade and Tore Supra, the numbers of bolometers must be enlarged to such an extent that the powerful technique of computer tomography, which is already being used in soft X-ray diagnostics /6/, can be applied. Owing to the rather restricted port access in most tokamaks, this requires bolometers of small size. The photolithographic manufacturing process for the gold-kapton-gold bolometer affords the potential to meet the requirements. It has already been possible to place complete arrays of micro-gold-meander bolometers on a single carrier foil /7-9/.

The bolometer presented in this report was designed with regard to small size, on the one hand, but also flexibility, reliability, accuracy and availability, on the other. If the dimensions of the gold pattern on the kapton foil are excessively reduced, problems arising from stray light, which originates at the viewing slits of

the foil mounting (see Sec. 8), and from self-heating due to the bolometer bridge current become severe. The biggest problem, however, is cross-talk between different detectors within the array /10/. The number of four bolometers constituting the present modules was chosen to make it possible both to build up one or two-dimensional arrays containing an arbitrary number of detectors and to replace only part of the arrangement for maintenance and repair.

The bolometer electronics is based on the well-known principle of an ac-excited ohmic bridge circuit (the bolometer module) with synchronous demodulation and filtering (see Fig. 12). This scheme was proposed by P. Betzler and F. Mast for a bolometer system because of its inherent advantage over a dc system.

In such a system the effects of dc drifts and the common-mode impact on the signal due to magnetic fields or other sources are expected to be minimized. Shielding problems will not be as severe as in a dc system. This not only influences the layout of the modules but also allows the use of cheaper cabling.

Disadvantages of an ac system: additional hardware is necessary (pulse generator, synchronous demodulator, sine generator).

2. Basic features of the bolometer

A schematic display of the bolometer design is given in Fig. 1. The design is based upon the same ideas underlying the first bolometer of this type /2/ used in the ASDEX experiment. A several μm thick gold layer absorbs the plasma radiation. The subsequent temperature rise of the bolometer foil causes a linear increase of the resistance value of a gold resistor layer in the $\text{k}\Omega$ range. A $7.5 \mu\text{m}$ thick kapton foil provides sufficiently strong thermal coupling as well as electrical insulation between the absorber and resistor. The rear surface of the irradiated part of the bolometer foil is completely and uniformly covered by the gold resistors, which are meander-like in shape (Fig. 2). The manufacturing process employs the photolithographic technique as an essential element.

The spatial separation of the absorber and the resistor layer allows separate adaptation of their properties, such as thickness, to the experimental requirements. On the one hand, the bolometer foil should be as thin as possible to endow it with a high sensitivity and a short response time (see Sec. 6), but, on the other, the absorber thickness must yield a sufficient stopping power to soft X-rays (Sec. 3), and the 7.5 μm thickness of the kapton foil is necessary to make the bolometer robust and reliable. In contrast, the dimensions of the gold conduction path are extremely small (Sec. 4), resulting in a rather high resistance value per unit area of the kapton foil, a quantity which is linearly correlated to the bolometer response to radiation.

When bolometers are miniaturized and arrays of them are placed on one kapton foil, two main problems arise. The first one is the efficient removal of heat, due to self-heating and radiation absorption, without inducing cross-talk between different channels. The second one is the decrease of the bolometer response to radiation in the low-frequency range owing to the smaller cooling-time constant (Sec. 6). A solution to both problems was given by the following change in the bolometer design /8,9/: An additional gold layer surrounding each absorber, called the heat resistor, delays the heat conduction from the absorber layer to the voluminous gold thermal-contact layer, on which a massive metallic cooling plate presses (Fig. 1). All three layers, the radiation absorber, the heat resistor and the thermal-contact layer can be formed by photo-etching a three-dimensional gold pattern on the front surface of the bolometer foil.

It is an approved and successful design feature /2/ to put a second so-called reference bolometer, shielded against the measured radiation, immediately next to its respective bolometer (Fig. 3) and to subtract the two bolometer signals by means of a bridge circuit (Fig. 2). Background noise signals are efficiently suppressed by this method. A modified version of the original bolometer used in JET demonstrated that an offset drift of the bolometer signal due to heating of the foil support during long-pulse plasma discharges can be compensated

by strong thermal coupling between the foil support of the bolometer and reference bolometer /2/. This concept has been retained and realized by means of the metallic cooling plate contacting all bolometers and reference bolometers on the kapton foil (Sec. 8).

Main requirements for the multi-bolometer module are:

- The heat transition from each individual thermal-contact layer to the cooling plate is uniquely defined to ensure that all bolometers have identical cooling-time constants.
- For the same reason the viewing slits cut into the cooling plate are shaped in such a way that they are not a source of stray light, that they generally do not limit the viewing range defined by a separate protruding aperture, that they do not allow radiation to impinge on the heat-resistor layers and thus vary the cooling-time constants.
- All bolometers in an alignment of multi-bolometer modules are equidistantly spaced.

A first design of a four-bolometer module /8/ did not satisfy all these stringent requirements. A completely new design was therefore necessary, which is presented in this report.

3. The absorber layer

The area required by the dimensions of the gold meander is 6 mm^2 (Sec. 3). The rectangular shape of the absorber reflects the symmetry of the diagnostic arrangement in the tokamak. The minor edge (1.5 mm) is orientated along the space coordinate, which has to be highly resolved, while the major edge (4 mm) is perpendicular to it. When the absorber thickness is $4 \text{ }\mu\text{m}$, this corresponds to an upper energy limit of photon absorption (1 % transmission) of about 5 keV (Fig. 4). Owing to the steep decay of the cross-section for photon attenuation between 5 and 10 keV, already about 50 % of 10 keV photons are not absorbed. Since in present-day tokamaks with strong auxiliary heating the temperatures in the hot plasma core may well exceed 5 keV, it is recommended that at least those bolometers which receive strong radiation are equipped with an absorber thickness of about $15 \text{ }\mu\text{m}$. Of course,

an increase of the bolometer thickness means a reduction of sensitivity (Sec. 6) and thus time resolution.

4. The electric resistor layer

In Ref. / 9 / it is proposed to give each of the four resistors of the bridge circuit the shape of a meander and to deposit them side by side on the kapton foil. It is optional to interweave the resistors R_1/R_2 and R_3/R_4 , the first pair representing the bolometer, the second one the reference bolometer (Fig. 2). The extremely small foil area occupied by the bridge and its symmetric outlay seem to be highly advantageous with respect to noise reduction and the application of an AC-bridge amplifier. The bridge output voltage at constant voltage supply doubles when both resistors R_1 and R_2 are irradiated and thus changed by ΔR each. The bridge sensitivity defined as total bridge resistance change per unit of absorbed radiation power stays constant, however. This is due to the fact that the resistance response ΔR of each individual meander is halved when their number on a prescribed foil area is doubled, because the resistance value R of each meander is halved and $\Delta R/R$ is constant.

If the two interwoven gold meanders are assumed to have a conduction path cross-section of $30 \times 0.05 \mu\text{m}^2$ and an area spread of $4 \times 1.5 \text{mm}^2$ their resistance is estimated at about $0.6 \text{k}\Omega$ each by extrapolation from ASDEX bolometer data /2/. Since the electrical properties of thin gold films drastically vary below $0.05 \mu\text{m}$, this thickness is a lower unit. Since the kapton foil commercially available exhibits a large area density of scratches, the proportion of defective bolometers is intolerable when the meander width is far below $30 \mu\text{m}$. The accuracy of the resistors has to be smaller than 2 %.

One main point should be brought out very clearly: The small bolometers will provide an improved time resolution not for thermodynamical reasons (Sec. 6), but for electronic ones. The small-sized bridge arrangement shown in Fig. 2 will reduce and compensate extremely well the pick-up of background noise even with a DC amplifier. But the reduction of the bolometer size allows the application of an AC-bridge

amplifier (50 Hz₂) because the capacitive resistance of the 6 mm² bolometer foil, a value which is directly proportional to the bolometer area, is about 125 kΩ and can thus be neglected. The AC bridge operates far off the low-frequency range where noise spectra typically occurring in tokamaks are located.

5. The heat-resistor layer

The question whether a heat-resistor layer as suggested in Ref. /8,9/ is actually needed in all cases is discussed in Sec. 6. But since it is desirable to have a free design parameter at one's disposal, the bolometer treated in this report is equipped with a heat-resistor layer.

The geometric dimensions of the heat-resistor layer determine the time constant τ_c of the heat conduction losses from the absorber layer to the thermal-constant layer, which is at the reference bolometer temperature:

$$(1) \quad \tau_c = \frac{(C_{Abs} + \frac{1}{2} C_{res}) \cdot l_{res}^2}{K \cdot V_{res}^A}$$

K is the thermal conductivity of gold, l_{res} is the resistor length, C_{Abs} is the total heat capacity of the absorber area, C_{res} is the total heat capacity of the heat resistor layer and V_{res}^A is the gold volume of the heat resistor layer. With a thickness of the gold heat resistor layer $d_{res} = 0.1 \mu\text{m}$ one obtains

$$\tau_c = 186 \text{ ms.}$$

This is much longer than the temperature equalization time of the absorber layer amounting to about 7 ms, which ensures a uniform temperature distribution across the absorber surface if the bolometer surface is uniformly illuminated. Equation 1 is, of course, only valid in vacuum surroundings and when the heat-resistor layer is not heated by incident radiation.

The value of K is experimentally determined from the measured cooling time of the ASDEX bolometer /4/, where the 4 μm thick gold absorber

layer is connected directly to the cooling body, i.e. the absorber and the heat-resistor layer are identical.

6. Frequency response, time constants and signal estimate

Generally, the thermal behaviour of the three-layer bolometer (gold absorber - kapton foil - gold resistor) is described by 3-dimensional heat-conduction theory. The heat-transfer time through the kapton foil is about 100 μ s and is thus much smaller than the other relevant time constants (see below). For that reason the heat-conduction equations are reduced to two space coordinates. The heat-transfer time is associated with a time delay of the bolometer response to a radiation pulse and is therefore called response time. In Ref. /2/ it is shown that even a one-dimensional analysis is a sufficiently good approximation in the two cases of constantly uniform or cosine temperature distributions on the bolometer surface. In the one-dimensional model the temperature rise δ averaged over the bolometer surface, the quantity which is measured by the meander resistor, obeys the equation

$$(2) \quad P = C \left(\frac{d\delta}{dt} + \frac{\delta}{\mathcal{T}_c} \right)$$

P is the radiation power observed by the bolometer, C is the heat capacity and \mathcal{T}_c is the cooling-time constant of the three-layer foil.

Anyone not very familiar with bolometer theory might assume that the cooling time \mathcal{T}_c is the lower limit of the time resolution and, secondly, that the bolometer sensitivity may be improved by a larger cooling time .

As Fig. 7a shows, the time resolution of the radiation power measurement by application of eq. 2 can be of the order of milliseconds when the cooling time amounts to almost two hundred milliseconds, and the time resolution is mainly determined by the electronic or numerical integration constant in order to smooth the noise signal. However,

Fig. 7b shows that the quantitative accuracy of eq. 2 deteriorates if the required time resolution of the measurement is an order of magnitude lower than the cooling-time constant and, thus, the time evolution of the spatial temperature distribution on the bolometer surface affects the bolometer signal.

From eq. 2 it follows that the frequency response of the bolometer is given by

$$(3) \quad \delta(\omega) = \frac{P(\omega)}{C} \times \frac{\mathcal{T}_c}{\sqrt{1 + \omega^2 \mathcal{T}_c^2}} .$$

At fixed radiation power amplitude $P(\omega)$ the temperature amplitude $\delta(\omega)$ is proportional to the reciprocal value of the heat capacity C , indicating that the bolometer sensitivity is reduced over the entire range of the spectrum when the thickness of the absorber is enlarged (see discussion in Sec. 3).

The frequency response given by eq. 3 is plotted in Fig. 8 for different values of \mathcal{T}_c . At very low frequencies ($\omega \mathcal{T}_c \ll 1$) the response grows linearly with \mathcal{T}_c :

$$(4) \quad \delta(\omega) = \frac{P(\omega)}{C} \times \mathcal{T}_c .$$

In contrast, in the high-frequency approximation ($\omega \mathcal{T}_c \gg 1$) the temperature signal is independent of \mathcal{T}_c :

$$(5) \quad \delta(\omega) = \frac{P(\omega)}{C} \times \frac{1}{\omega} .$$

This means that the signal-to-noise ratio of bolometers with cooling times longer than 20 ms is not increased at frequencies above 20 Hz when an additional heat-resistor layer raises the cooling time (Fig. 8).

If small bolometers are not fast, i.e. not capable of measuring the higher radiation frequencies because the signal-to-noise ratio is insufficient, then an increase of \mathcal{T}_c by adding the heat-resistor layer ensures that at least the low-frequency part of the radiation spectrum is measured, as Fig. 8 shows. In contrast, if small bolometers are fast,

i.e. owing to excellent design of the bridge circuit the noise is reduced to such a level that the range of measurement is extended to high radiation frequencies ($\gg 50$ Hz), then low frequencies can be measured even better since their signal-to-noise ratio can be further improved by numerical smoothing routines. In such a case there is no need at all to install a heat-resistor layer; it would even bear disadvantages: The flat response over a wide frequency range is lost. The dynamic range is limited owing to overheating of the bolometer foils and saturation of the preamplifiers. The bridge output signal becomes nonlinear for large signals. The accuracy of eq. 2 becomes worse owing to the slow decay of distortions of the original temperature distribution on the bolometer surface (Fig. 7b).

The tokamaks PULSATOR, ASDEX, JET and ASDEX Upgrade generate a wall power load due to radiation which is of the order of $W \cdot cm^{-2}$ for ohmic discharges, independently of their size. If the poloidal plasma cross-section is divided into 20 viewing chords, the bolometers receive a radiation intensity of typically $2 \text{ mW} \cdot cm^{-2}$. Hence, the stationary temperature response of a bolometer with a cooling time of $\mathcal{T}_c = 180 \text{ ms}$ is about 0.2° C . If a bridge voltage of 5 V and a resistance value of $0.6 \text{ k}\Omega$ are assumed (Sec. 4) the resistance changes by 0.3Ω and the bridge output signal is of the order of 1 mV . In the worst case, if the noise level of the new bridge circuit is not superior to the old one used in ASDEX and JET, we have to adjust the cooling time \mathcal{T}_c to values between 100 and 200 ms (curves 1 and 2 of Fig. 8) by means of the heat-resistor layer. We are then on the safe side for radiation frequencies below 20 Hz. This value agrees with the experience gained in JET, where bolometric data from ohmic discharges with low radiation levels can only be sampled with 50 Hz.

But if first tests prove that the new AC-bridge circuit /11/ suppresses the noise level by orders of magnitude better than the old DC circuit, then a value of \mathcal{T}_c between 10 and 20 ms (curves 4 and 5 of Fig. 8) may be appropriate. But, since such \mathcal{T}_c values can be obtained by absorbers which have slightly enlarged sizes (see Sec. 4) of $2 \text{ mm} \times 4 \text{ mm}$ ($\mathcal{T}_c = 11 \text{ ms}$), $2.5 \text{ mm} \times 4 \text{ mm}$ ($\mathcal{T}_c = 16 \text{ ms}$) or $3 \text{ mm} \times 4 \text{ mm}$ ($\mathcal{T}_c = 20 \text{ ms}$)

and which are contacted directly by the cooling body like the ASDEX bolometer /2/, the heat-resistor layer could be omitted in such a case.

When we have to deal with rather strong radiation intensities in cases of uncollimated viewing (only in the poloidal plane) and auxiliary heating, bolometer foils with $\tau_c = 180$ ms show a temperature increase of up to 200° C during single plasma discharges. So-called 2π bolometers with no collimation at all which are irradiated by up to $10 \text{ W}\cdot\text{cm}^{-2}$ would certainly be destroyed. If the $1.5 \text{ mm} \times 4 \text{ mm}$ bolometer foil having a cooling time of $\tau_c = 7$ ms (curve 6 of Fig. 8) is contacted directly by the cooling body and the heat-resistor layer is omitted, then it is suitable for even such an application (see Sec. 8).

7. The thermal-contact layer

The ASDEX bolometer foil /2/ has already been thermally contacted by a cooling body pressing on a thickened gold edge layer. The soft gold layer compensates the surface roughness of the cooling body, which is of the order of several μm . Hence, a strong and uniquely defined thermal coupling between the foil and the cooling plate is established. The thermal-contact layer of each bolometer is 19 mm^2 (Fig. 5) and $15 \mu\text{m}$ thick (Fig. 6). For reasons of mechanical stability it is advised not to exceed this thickness (see also Sec. 3). In our application case the thermal-contact layer cannot act as a cooling layer as was suggested in Ref. /9/. Firstly, typical plasma discharges last up to 50 times longer than the heat equalization through the heat-resistor layer. Secondly, the volume of the edge layer is only 3 times larger than that of a $15 \mu\text{m}$ thick absorber.

There is a gold-free gap between the thermal-contact layers of adjacent bolometers. It is designed in such a way that all bolometers of an alignment of four-bolometer modules are equidistant (Fig. 3). The gap ensures that the heat losses of the bolometers are transported exclusively to the cooling plate. The probability of heat conduction through the kapton foil is 5 orders of magnitude smaller.

8. The cooling plate, its aperture system and the mounting support

Four bolometers and four reference bolometers of the type described in the previous sections are arranged side by side on the kapton foil. They constitute a module with the dimensions $2.0 \times 3.3 \text{ cm}^2$ (Fig. 2).

The cooling plate consists of a 3 mm thick aluminium plate pressing onto the thermal-contact layers of all bolometers and reference bolometers of the module, and it thus acts as a heat sink. Immediately next to the location of the bolometers and reference bolometers its thickness is stepwise reduced to 0.6 mm, and in the case of the bolometers receiving radiation further steps cut into the material form a window slit (Fig. 9).

A residual thickness of 0.6 mm enables easy penetration of neutron and gamma radiation to the reference bolometer to compensate the major part of the background signal due to nuclear radiation by means of the bridge circuit. This is very important in tokamaks with D-T operation, such as JET (see Ref. /2/).

The step-like form of the window slits prevents stray light originating from the window-frames. The steps are typically 0.25 mm deep and 0.1 mm wide (Fig. 6) and they are shaped by spark erosion.

The slope of the envelope of the steps defines the viewing angle: it is $\pm 20^\circ$ in the direction of the bolometer alignment and $\pm 60^\circ$ perpendicular to it (Figs. 10 and 11). This means that in most practical cases the window-frames do not limit the viewing range of the bolometers. For example, in all known pin-hole cameras the viewing angles determined by the aperture common to all bolometers are smaller than $\pm 20^\circ$. A viewing angle of $\pm 60^\circ$ is even sufficient to use the bolometer as an uncollimated bolometer (see discussion in Sec. 6). "Uncollimated" means that the entire poloidal plasma cross-section, but only a 5 % segment of the toroidal circumference is viewed. The application of a four-element module as an uncollimated bolometer makes rough energy resolution and thus radiation source determination possible when the four detectors are equipped with suitable filters, e.g. LiF-glass and beryllium foils of different thickness /2,3/.

In order to shield the heat-resistor layer against radiation the window-frame overlaps the edge of the absorber layer. Thus 18 % of the absorber area is shaded (Figs. 6, 10 and 11). Considering also the manufacturing tolerances, it is an important conclusion that each bolometer including its window aperture must be calibrated by means of a standard radiation source. The method of square-wave excitation of the bolometer current and measurement of the bolometer response to this ohmic power pulse /2/ can merely be employed as an additional and relative calibration in order to record the long-term drift of the bolometer sensitivity.

The design of the mounting support is straightforward and Figs. 6, 9, 10 and 11 are self-explanatory. There is one point to be noted: The performance of the elastic contact pins gradually declines at temperatures of more than 200°C , a value which is well above the maximum vessel temperature of 150°C of ASDEX Upgrade and Tore Supra.

9. Components of bolometer electronics

(for an overview see Fig. 18).

A. Preamplifier (see Fig. 14)

The preamplifier covers two problems:

- i) the distance between the 4-channel bolometer module and the camac equipment typically exceeds 50 m. Signal cables of such a length would excessively load the bolometer bridge by the cable capacitance.
- ii) The individual bolometer shows an inherent ac output offset voltage due to tolerances in its resistive elements (1 to 5 %). This offset voltage would cause clamping of amplifier stages whenever high gain is needed.

Compensation of the offset signal

A portion of the bridge exciting signal is used for compensating the offset. Both signals (the bridge output signal and the counter-phased compensating signal) are added in a SUMMING AMP whose output is adjusted to a low, well-defined amplitude (use of a trimmer and a supporting LED). The phase of the bridge output signal is also matched

by a PHASE SHIFTER (trimmer and supporting LED).

Variable-gain amplifier stages

Two amplifier stages allow transmission of quite high signals via the cable to the "MAIN AMP". Gain switching is decoupled by optocouplers in order to prevent closed loops.

Output driver

Two output buffers (gain = 1) serve as drivers for long cables (up to 100 m of shielded quad cable).

Power supply

Power for the preamp is transferred from the "MAIN AMP" via the same quad cable by which the amplifier signal is sent to the "MAIN AMP" (use of the second "pair" of the quad).

Test of preamp

With the help of relays, a well-defined portion of the bridge excitation voltage (which is stabilized) can be fed to the input amp. This allows almost overall testing of the complete chain. The relays are operated via optocouplers.

B. "MAIN AMP" (see Fig. 15)

The "MAIN AMP" board represents a module which not only is useful for the bolometer system but can also be operated with other sensors, such as LVDT's, strain gauges and position sensors in a carrier frequency system. The board houses:

Input amp

Instrumentation amp type: gain can be selected by varying one resistor.

Synchronous detector

A type AD630 (Analog Devices) is used as demodulator. A synchronous control signal is derived from the SINE GENERATOR and fed to the AD630 via an optocoupler. The control signal can be delayed and reversed.

Summing amp and reset circuit

The "ZERO"-output level of the BESSEL FILTER is automatically set at an adjustable level upon a RESET TRIGGER from an external timer decoupled by an optocoupler.

The REST TRIGGER is applied immediately before the plasma pulse and the electronics stays "frozen" until a new reset command is sent. The RESET CIRCUIT consists of an 8-bit DAC for coarse adjustment, and a sample-and-hold circuit for fine adjustment. Both circuits produce a corrective dc current which is added to the demodulator output in the SUMMING AMP in order to achieve the desired output level.

Low-pass filter (see Fig. 16)

This filter is necessary in order to suppress the carrier frequency and to restore the modulation signal, which represents the desired information from the sensor.

A BESSEL characteristic was chosen for minimum signal distortion. The critical frequency of the filter determines the dynamic response of the system. This must be traded off against the maximum allowable carrier components in the output of the filter. Since this filter also serves as an anti-aliasing filter for the ADC, it should be ensured that the ADC's sampling rate is more than twice the critical frequency of the filter.

Isolation amp

Closed loops are avoided by using an ISOLATION AMP as a link to the CAMAC-ADC. The CURR-BROWN type 3650 was selected, which offers a quite high large-signal bandwidth (approx. 5 kHz) and good insulation capability (≥ 2 kV DC).

Power supply (see Fig. 17)

Power is supplied from a DC-DC CONVERTER which offers ± 18 V stabilized and ± 24 V non-stabilized. The total combined output current is limited to ≤ 500 mA. Oscillation is at ≈ 25 kHz (free run). External synchronization and switch-off are optional.

C. Bridge Supply Sine Generator (see Fig. 18)

The 4-channel bolometer module is supplied with a pure sine signal which is common to the four channels of the module. The generator has complementary outputs in order to minimize common-mode problems for the preamplifier input stage (see also Fig. 12).

The generator is controlled by an external square wave generator. The sine is derived from the square wave with the help of a bandpass. The bandpass suppresses harmonic contents of the square and minimizes low-frequency components (such as the 50 Hz line frequency).

A constantly operating control circuit stabilizes the amplitude of the bridge excitation directly at the bridge (no effect of long cables; the second pair of quad cables is used as a sensor pair for feedback of the actual amplitude at the bridge).

A SYNC signal is derived from the generator's output drivers for synchronization of the synchronous demodulators. Input and output square wave signals are decoupled by optocouplers.

Since the generator is floating, it needs a dc-dc converter of the same type as described above.

D. Control Equipment for a Complete 100-Channel System

Control of sine generators (see Fig. 19)

All BRIDGE SUPPLY SINE GENERATORS (25 generators in a 100-channel system) will be controlled by an external pulse generator system already developed for the JET BOLOMETER SYSTEM. It consists of a 10 MHz clock, a programmable pulse generator and two output drivers.

Control of gain (see Fig. 20)

Each of the 100 PREAMPS needs 4 bits for gain control. These bits are stored in addressable LATCH cards (one card for one channel). A special CAMAC memory (SERIMEM, ASDEX development) will be loaded with data and channel addresses. The content of this memory will be sent serially to the LATCHES upon a trigger. Thus, the loading of the channels is not directly done by the computer, which is free for other operations and is only occasionally needed for updating the data.

Status Report

At present a prototype system consisting of

4 PREAMP	cards
4 MAIN AMP	cards
1 GENERATOR	card
1 10-MHz CLOCK	card
1 PROG. PULSE GEN.	card
1 OUTPUT DRIVER	card
5 DC-DC CONVERTER	cards

which is suitable for one 4-channel bolometer module is being tested in the laboratory. We use 100 m telephone cables (shielded quads) as lines between the MAIN AMP and PREAMP and

between the GENERATOR and BOLOMETER MODULE.

Simple shielded-pair cables connect the PREAMPS with the BOLOMETER MODULE (≤ 10 m in length).

The system shows the expected performance. At present it is operated at its maximum carrier frequency (≈ 50 kHz) using a "dummy bolometer"; input noise (10 kHz BESSEL LOW PASS) is less than 1 μ V (RMS).

Droop rate of the sample + hold is less than 2.5 mV within 20 sec.

Physical size of cards: all EUROCARDS 100 x 220 mm; 30 mm in width

dc-dc converter: EUROCARD 100 mm x 80 mm;

30 mm in width;

Layout: printed circuit, inexpensive shielding.

9. Summary and outlook

A new multi-bolometer module for application in high-temperature plasma diagnostics has been designed. At first, it will be used in the tokamaks ASDEX Upgrade and Tore Supra. Its design employs features from different stages of bolometer development (Refs. /2, 8, 9/.)

The fundamental part of the design is based upon ideas which proved to be successful in the original ASDEX bolometer /2/ and which endow also the new bolometer with excellent properties: It is extremely robust and reliable, and it can be baked to between 200 and 300^o C.

The bolometer is insensitive to nuclear radiation damage up to radia-

Status Report

At present a prototype system consisting of

4 PREAMP	cards
4 MAIN AMP	cards
1 GENERATOR	card
1 10-MHz CLOCK	card
1 PROG. PULSE GEN.	card
1 OUTPUT DRIVER	card
5 DC-DC CONVERTER	cards

which is suitable for one 4-channel bolometer module is being tested in the laboratory. We use 100 m telephone cables (shielded quads) as lines between the MAIN AMP and PREAMP and

between the GENERATOR and BOLOMETER MODULE.

Simple shielded-pair cables connect the PREAMPS with the BOLOMETER MODULE (≤ 10 m in length).

The system shows the expected performance. At present it is operated at its maximum carrier frequency (≈ 50 kHz) using a "dummy bolometer"; input noise (10 kHz BESSEL LOW PASS) is less than 1 μ V (RMS).

Droop rate of the sample + hold is less than 2.5 mV within 20 sec.

Physical size of cards: all EUROCARDS 100 x 220 mm; 30 mm in width

dc-dc converter: EUROCARD 100 mm x 80 mm;

30 mm in width;

Layout: printed circuit, inexpensive shielding.

9. Summary and outlook

A new multi-bolometer module for application in high-temperature plasma diagnostics has been designed. At first, it will be used in the tokamaks ASDEX Upgrade and Tore Supra. Its design employs features from different stages of bolometer development (Refs. /2, 8, 9/.)

The fundamental part of the design is based upon ideas which proved to be successful in the original ASDEX bolometer /2/ and which endow also the new bolometer with excellent properties: It is extremely robust and reliable, and it can be baked to between 200 and 300^o C.

The bolometer is insensitive to nuclear radiation damage up to radia-

tion doses of about 5×10^9 rad. The calibration data should be highly reproducible and stable in time. A (relative) calibration can be performed 'in situ' by square-wave excitation of the bolometer current and analysis of the self-heating vs time. The bolometer has a linear response, and the rather simple analytic formula applied is sufficiently accurate for signal analysis. Ambient interference signals will be efficiently reduced by pairing next neighbours of bolometers, half of them shielded against radiation in an electronic AC-bridge circuit (50 kHz). The size of a four-bolometer module is $2.0 \times 3.3 \text{ cm}^2$.

Some questions still remain open and they have to be answered partly by the project management of ASDEX Upgrade and Tore Supra, partly by prototype tests. The energy range of the plasma radiation expected will determine the absorber thickness. First measurements with a prototype, partly performed on an existing tokamak (e.g. ASDEX), will answer two main questions: How large is the cooling-time constant of the bolometer foil and does it agree with the estimate given in Sec. 5. Secondly, what is the minimum noise ratio in the low-frequency range of plasma radiation (see Fig. 8)? Both answers will decide whether a heat-resistor layer is actually needed and how it is to be dimensioned. An absolute calibration method using a standard radiation source is to be established and the quality as well as the reproducibility of the step-like viewing slits in the cooling plate are to be tested.

Concerning the electronics, the following steps have to be taken before manufacturing the final system:

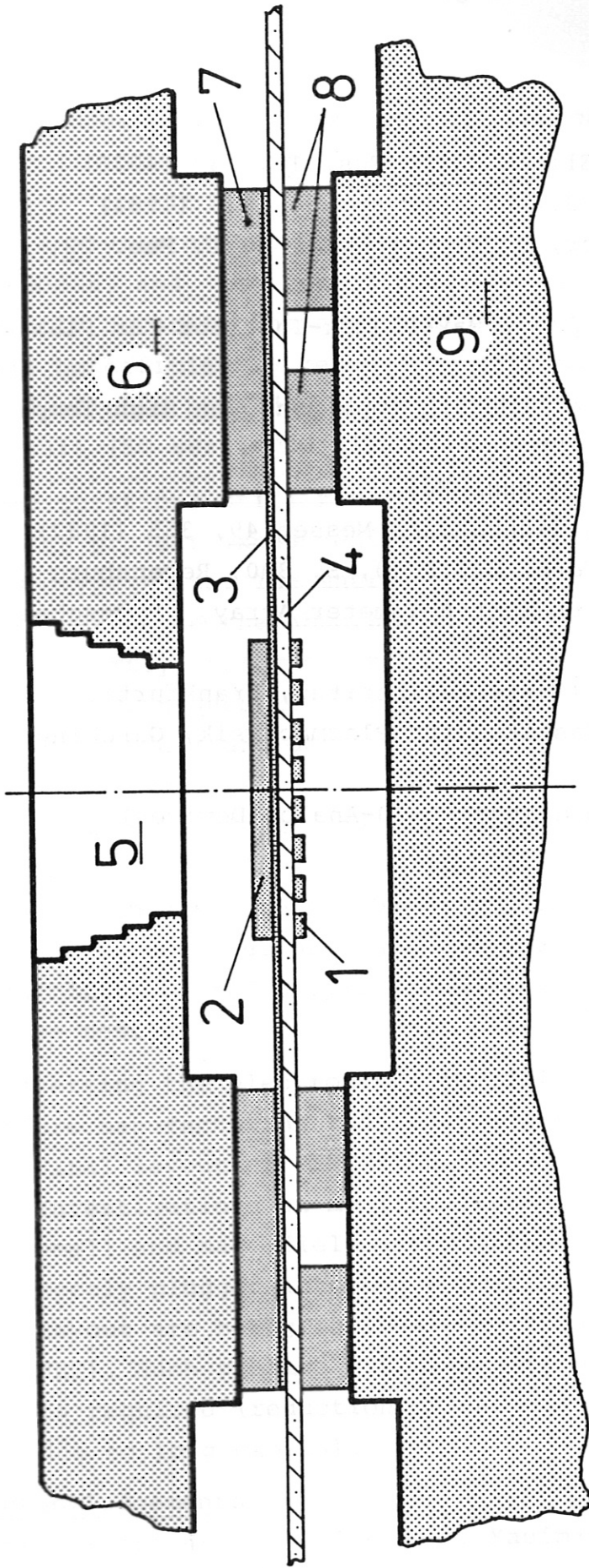
- Final layout of GENERATOR card and MAIN AMP card.
- Investigations on miniaturization of individual PREAMPS to achieve small and mag. field transient-proof modules which could be directly plugged into the BOLOMETER MODULES (preamps with similar layout are being successfully used in the soft X-ray system at JET). Such preamps are necessary whenever fast transient response is required (reduction of capacitive load on the bolometer module due to long cables).

Acknowledgements

The authors are grateful to M. Kaufmann and H. Röhr for support and encouragement. They are indebted to P. Betzler for stimulating and helpful discussions.

References

- /1/ H. Hsuan, K. Bol, R.A. Ellis, Nucl. Fus. 15, 657 (1975)
- /2/ E.R. Müller, K.F. Mast, J. Appl. Phys. 55, 2635 (1984)
- /3/ E.R. Müller, K. Behringer, H. Niedermeyer, Nucl. Fus. 22, 1651 (1982)
- /4/ E.R. Müller, Report IPP 3/56, Max-Planck-Institut für Plasma-physik, Garching (1980)
- /5/ K.F. Mast et al., Proc. of the 5th Top. Conf. on High Temp. Pl. Diagn., Tahoe City, 1984
- /6/ P. Smeulders, submitted to Nucl Fus.
- /7/ R. Hartmann, M. Selders, Technisches Messen 49, 355 (1982)
- /8/ K.F. Mast, R. Betzler, Verh. DPG P 40, S. 390, Regensburg (1983)
- /9/ P. Betzler, Micro Multi Element Bolometer Array, Deutsches Patent P 34 08 724.9
- /10/ R. Hartmann. M. Selders (Battelle Institut, Frankfurt), P. Betzler (Max-Planck-Institut für Plasmaphysik, Garching) private communication
- /11/ Balanced Modulator (Demodulator AD630-Analog Devices)



- 1. gold-meander resistor
- 2. gold absorber layer
- 3. golden heat-resistor layer
- 4. kapton carrier foil
- 5. viewing window
- 6. aluminum cooling plate
- 7. golden thermal-contact layer
- 8. conduction path
- 9. mounting support

Fig.1 Schematic display of the bolometer design

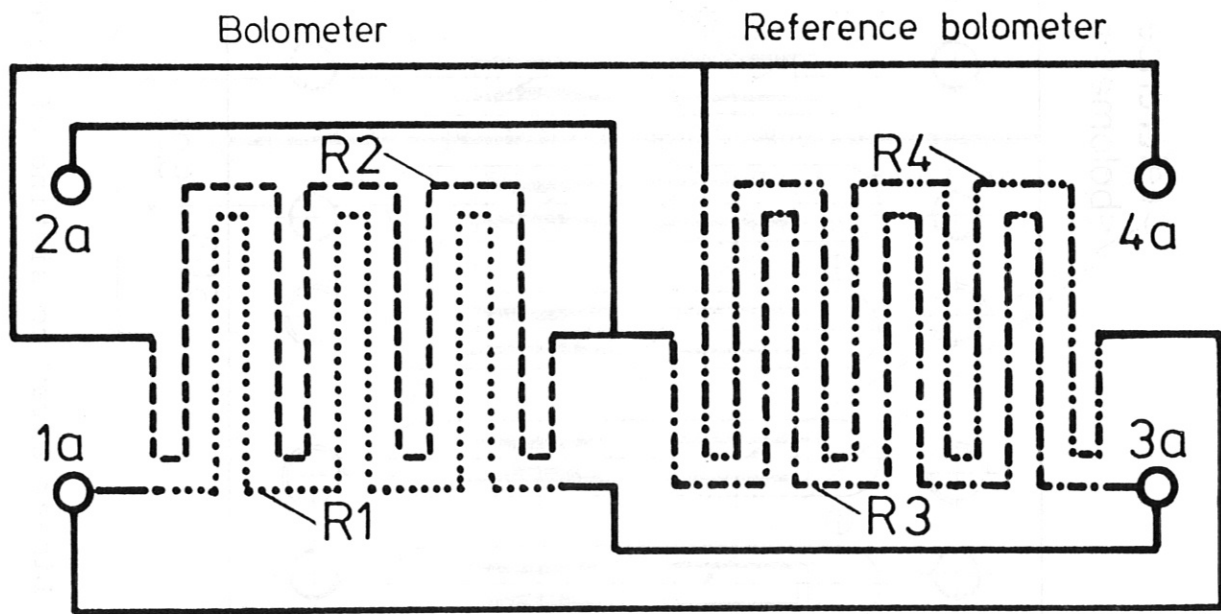
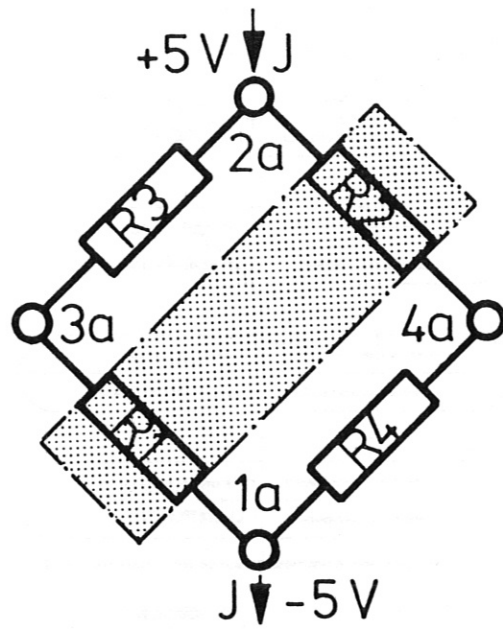


Fig.2 Arrangement of the bridge circuit on the kapton foil , schematic (from Ref. /9/)

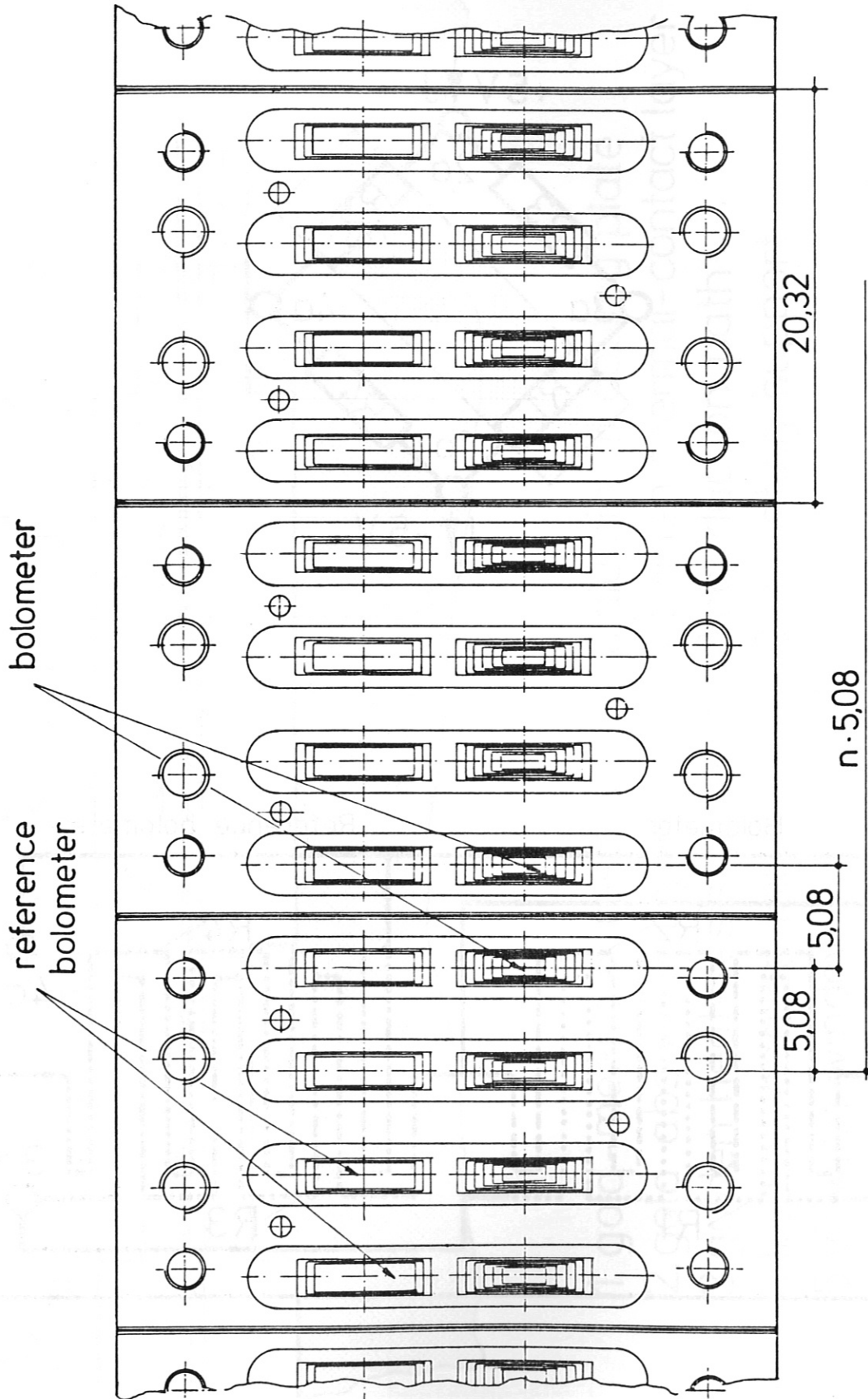


Fig.3 Linear array consisting of several four-bolometer modules

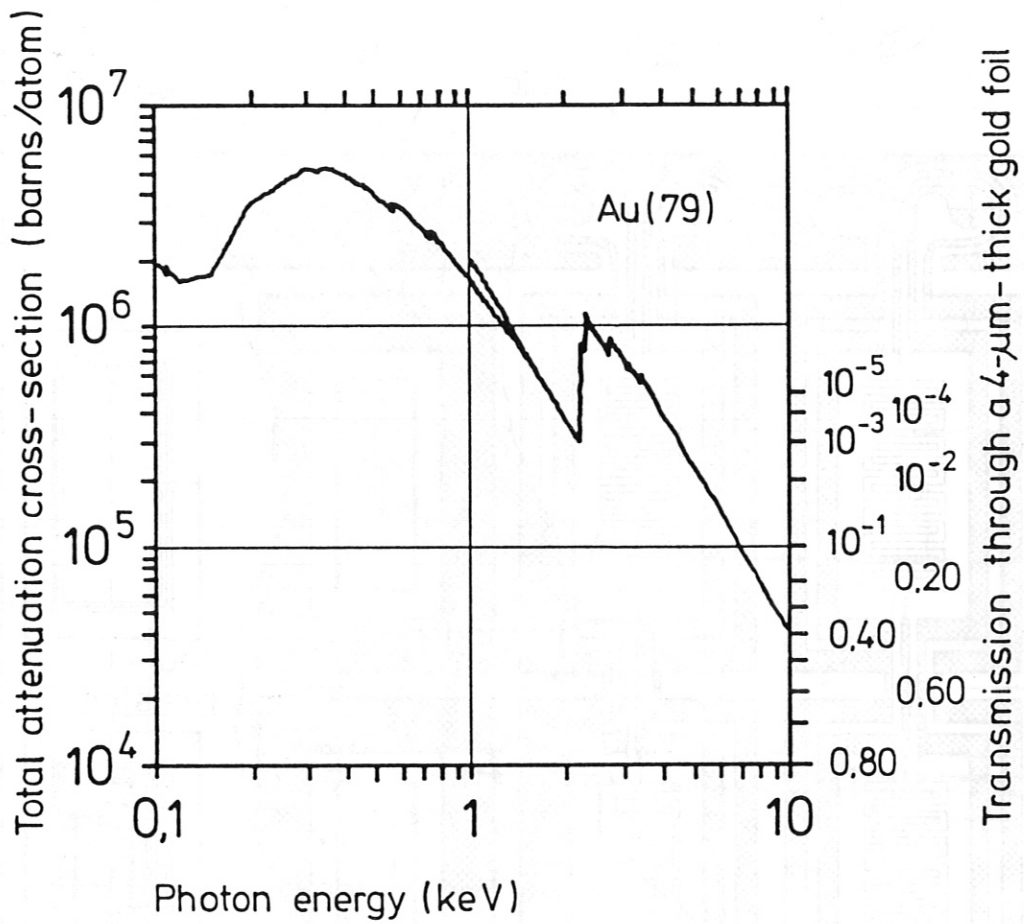


Fig. 4 Total photon attenuation cross-section of gold and transmission through a 4- μ m thick gold foil in the photon energy region 0.1 to 10 keV (from Ref. /4/)

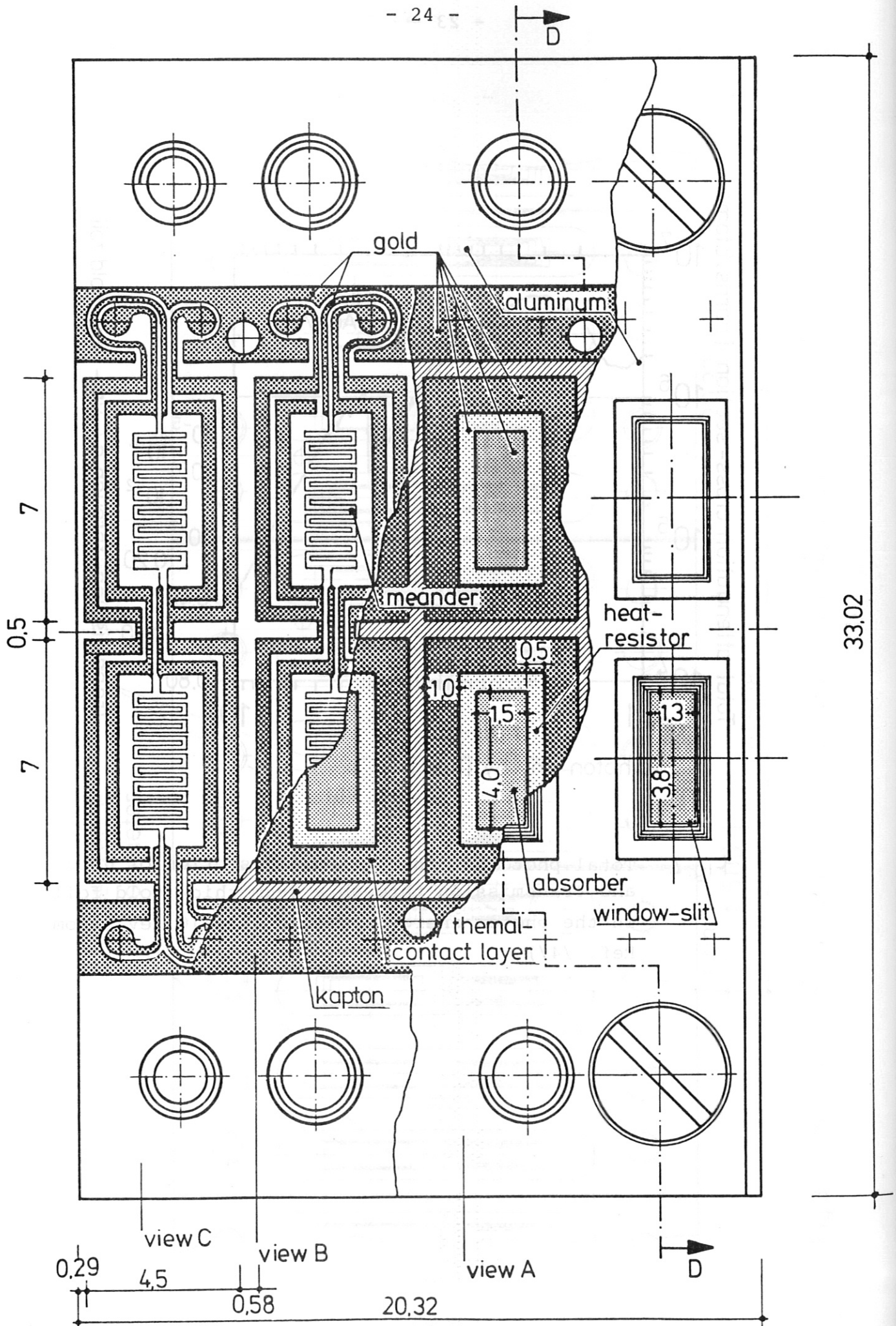


Fig.5 Top view of the bolometer foil

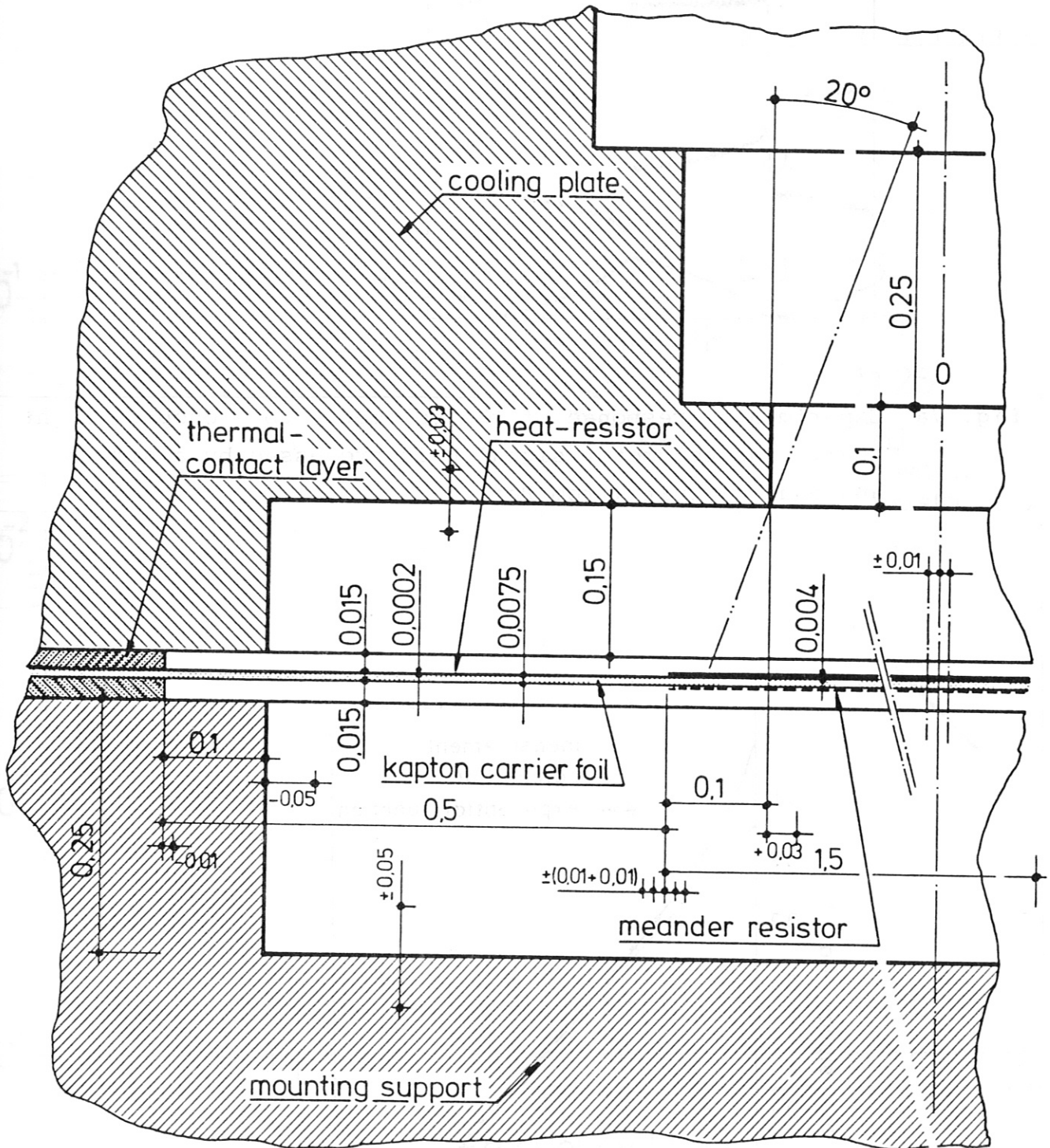


Fig. 6 Blown-up section of Fig. 9, giving a side view of the bolometer foil, the cooling body and the step-like window slit

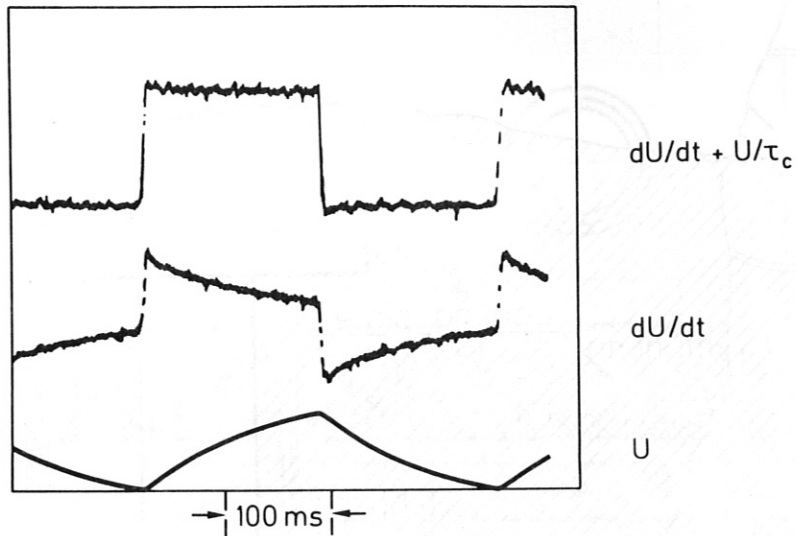


Fig. 7a Experimental response of the bolometer to a chopped light beam. The bolometer signal U is processed by a simple analogue circuit (from Ref. /2/)

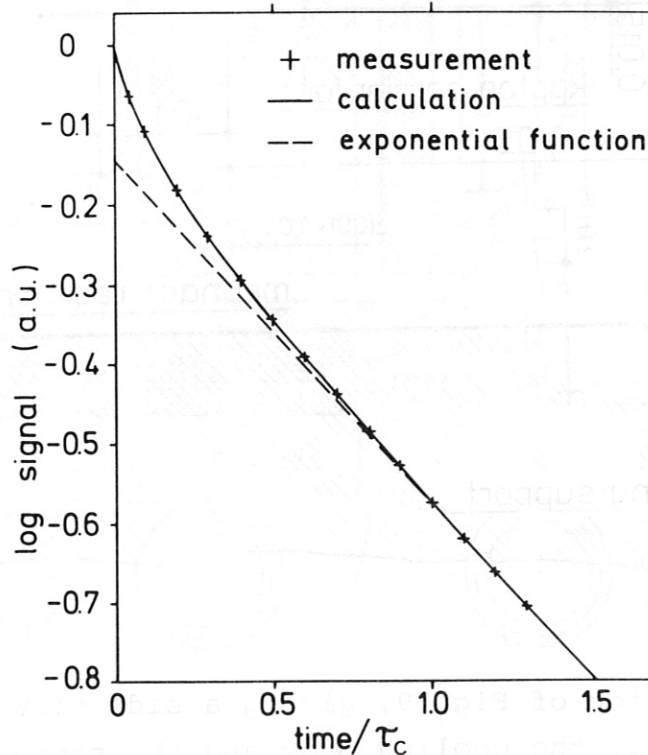


Fig. 7b Comparison of the calculated cooling-down curve, considering the two-dimensional temperature distribution across the bolometer surface, with the measured one. Both slightly deviate from an exponential function predicted by eq. 2 (from Ref. /2/)

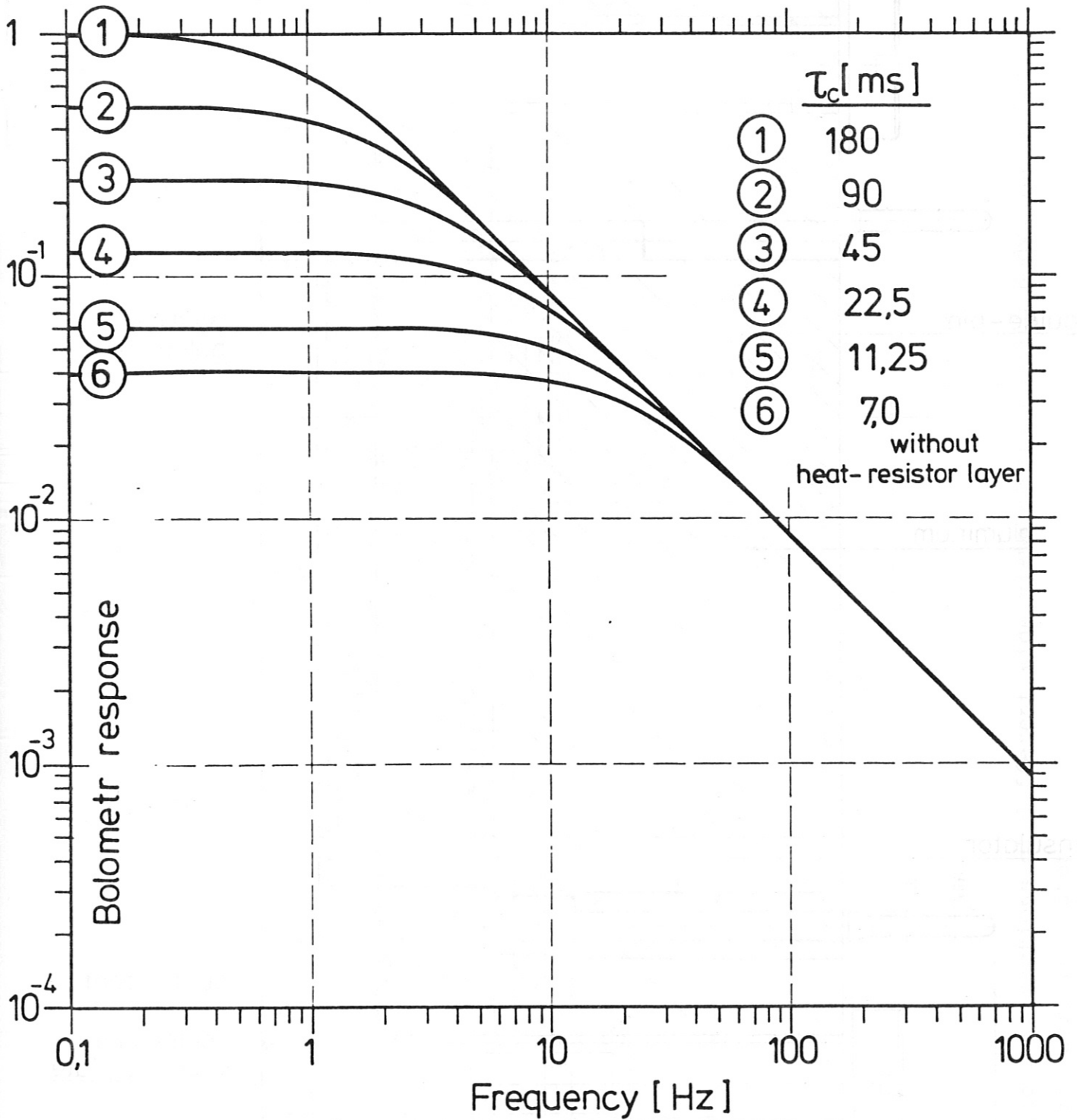


Fig. 8 Frequency response of the bolometer foil, according to eq. 3, for different values of the cooling time τ_c .

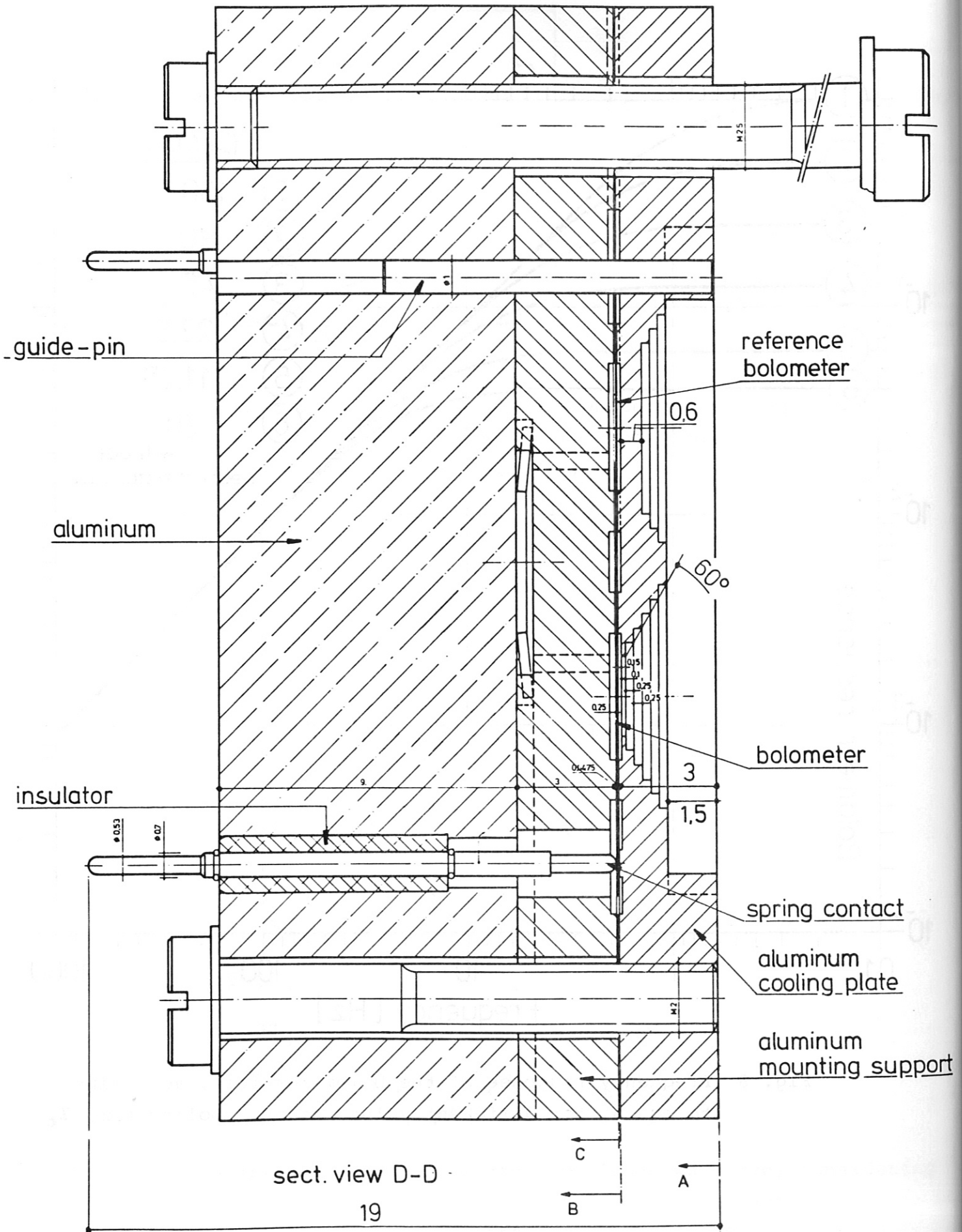


Fig.9 Side view of the bolometer module

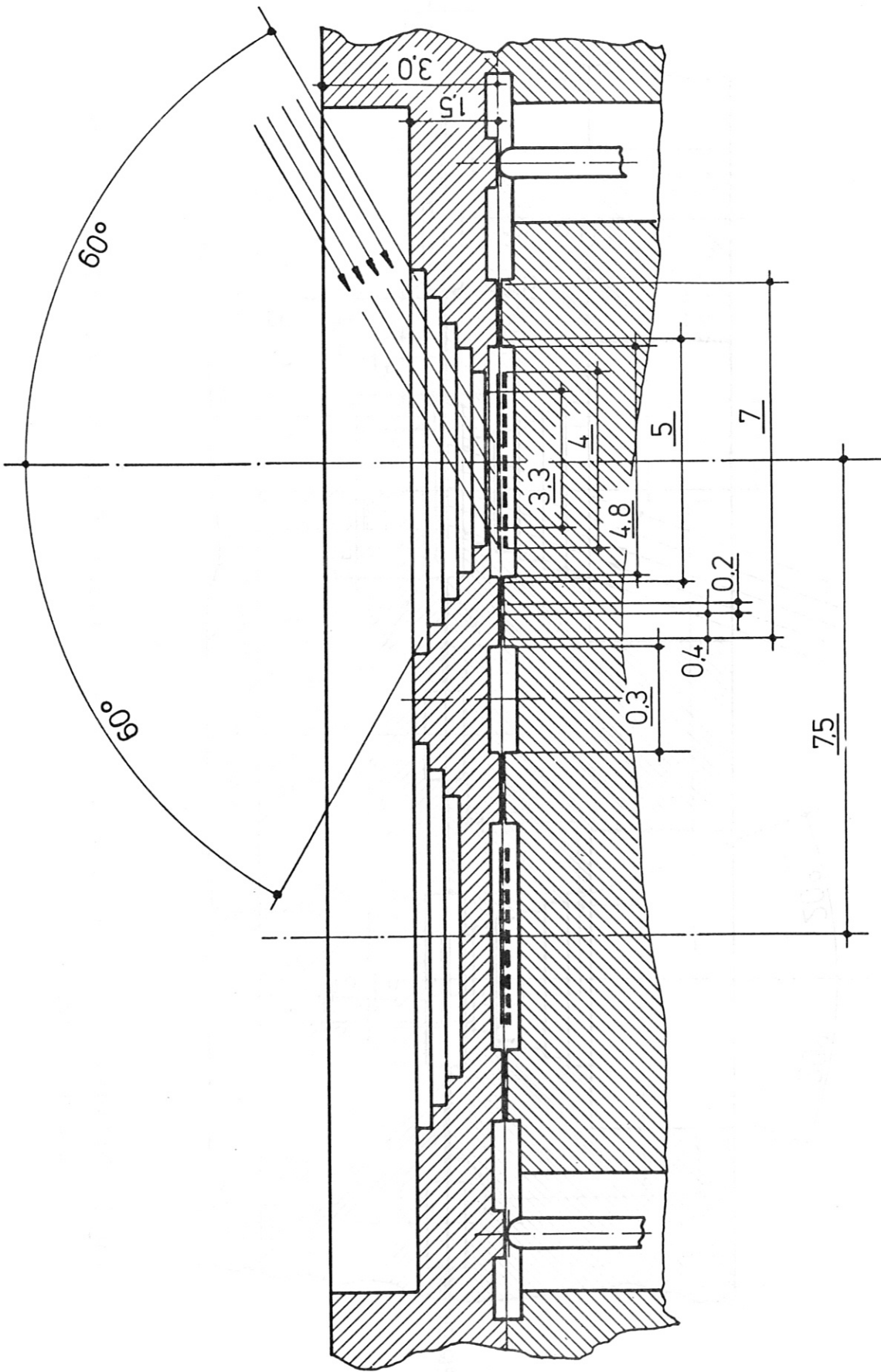


Fig.10

Fig. 10 Blown-up sections of different side views of the cooling body, including its aperture system

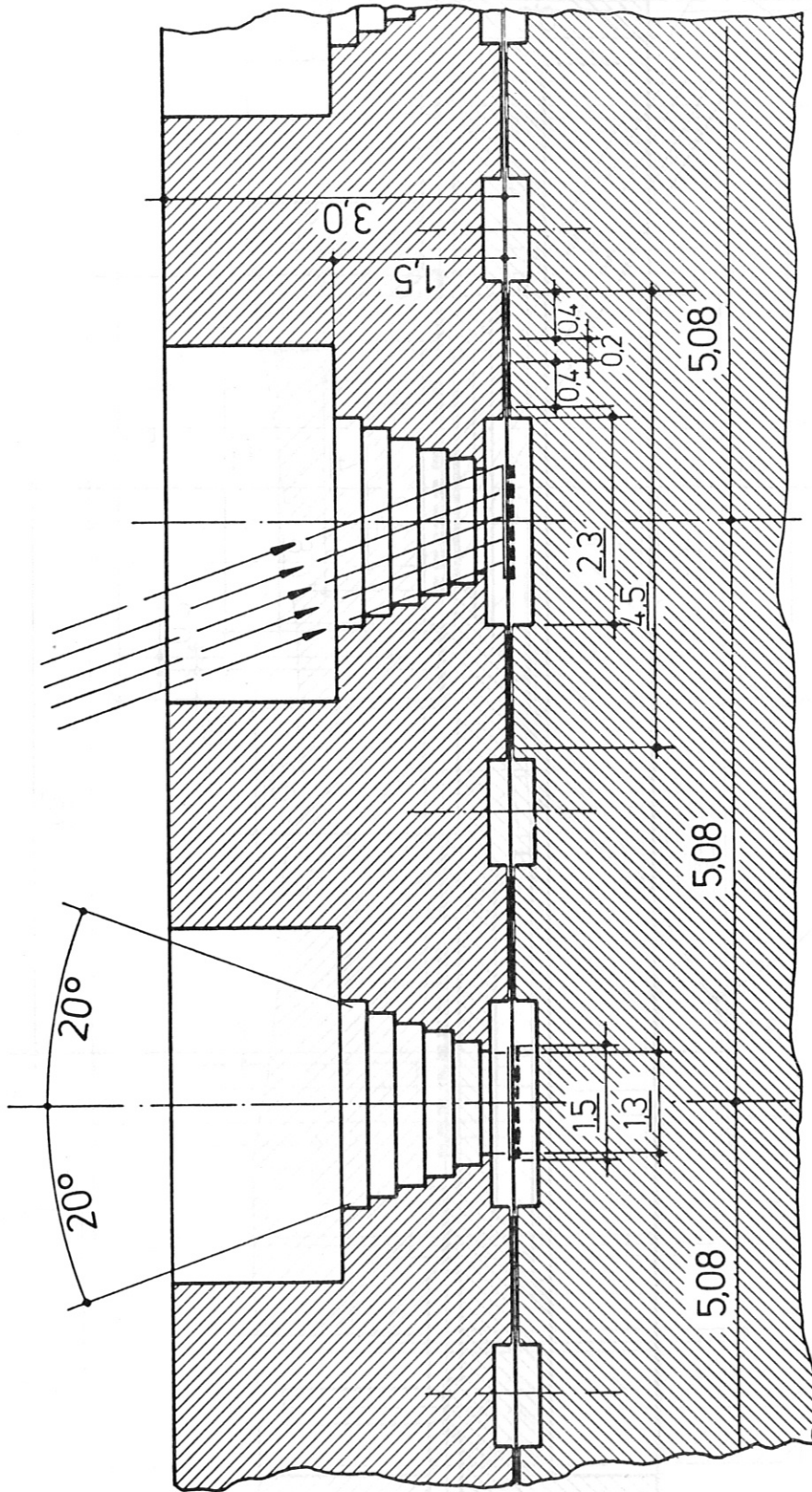


Fig.11 Blown-up sections of different side views of the cooling body, including its aperture system

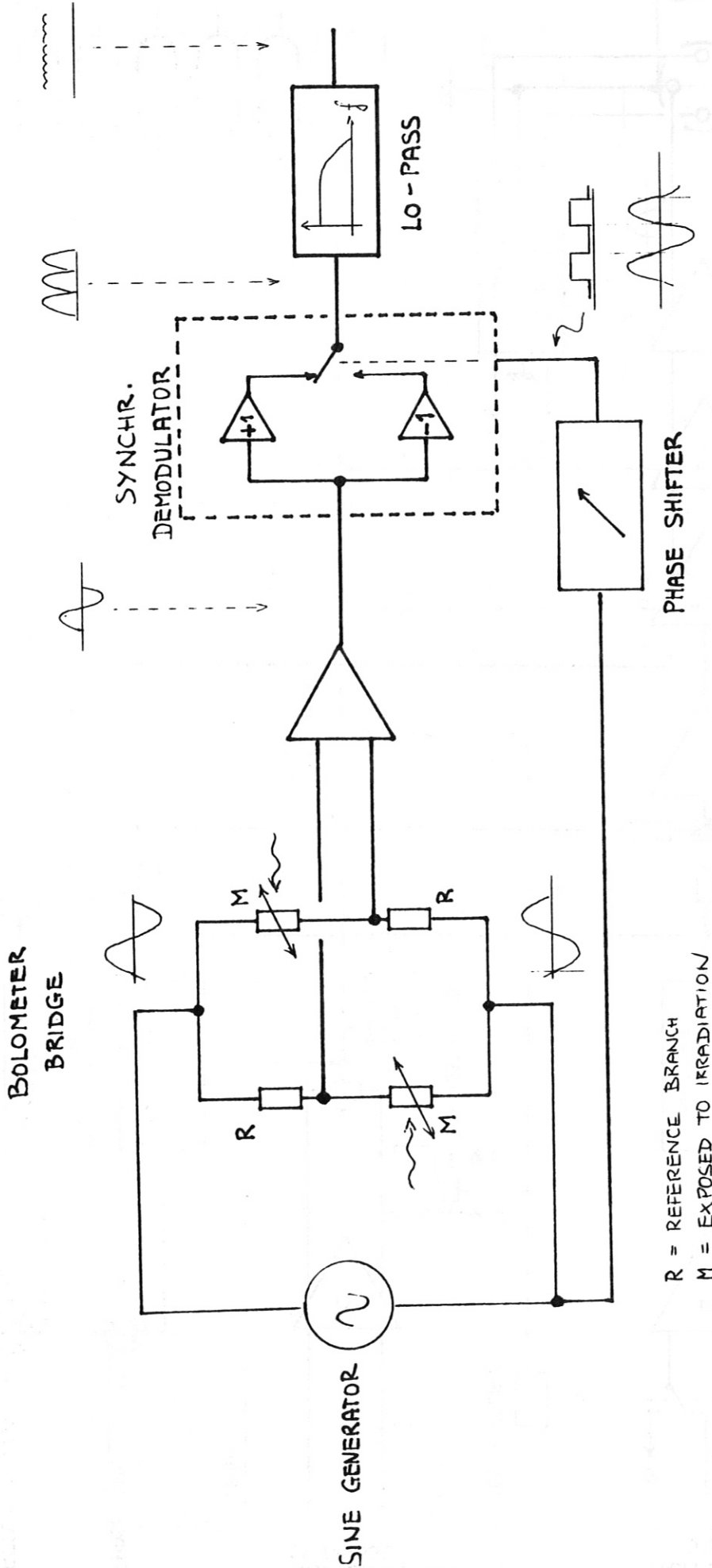


Fig. 12 AC excited bridge system with synchronous demodulator and low pass filter

11/85 *SLA*
IPP

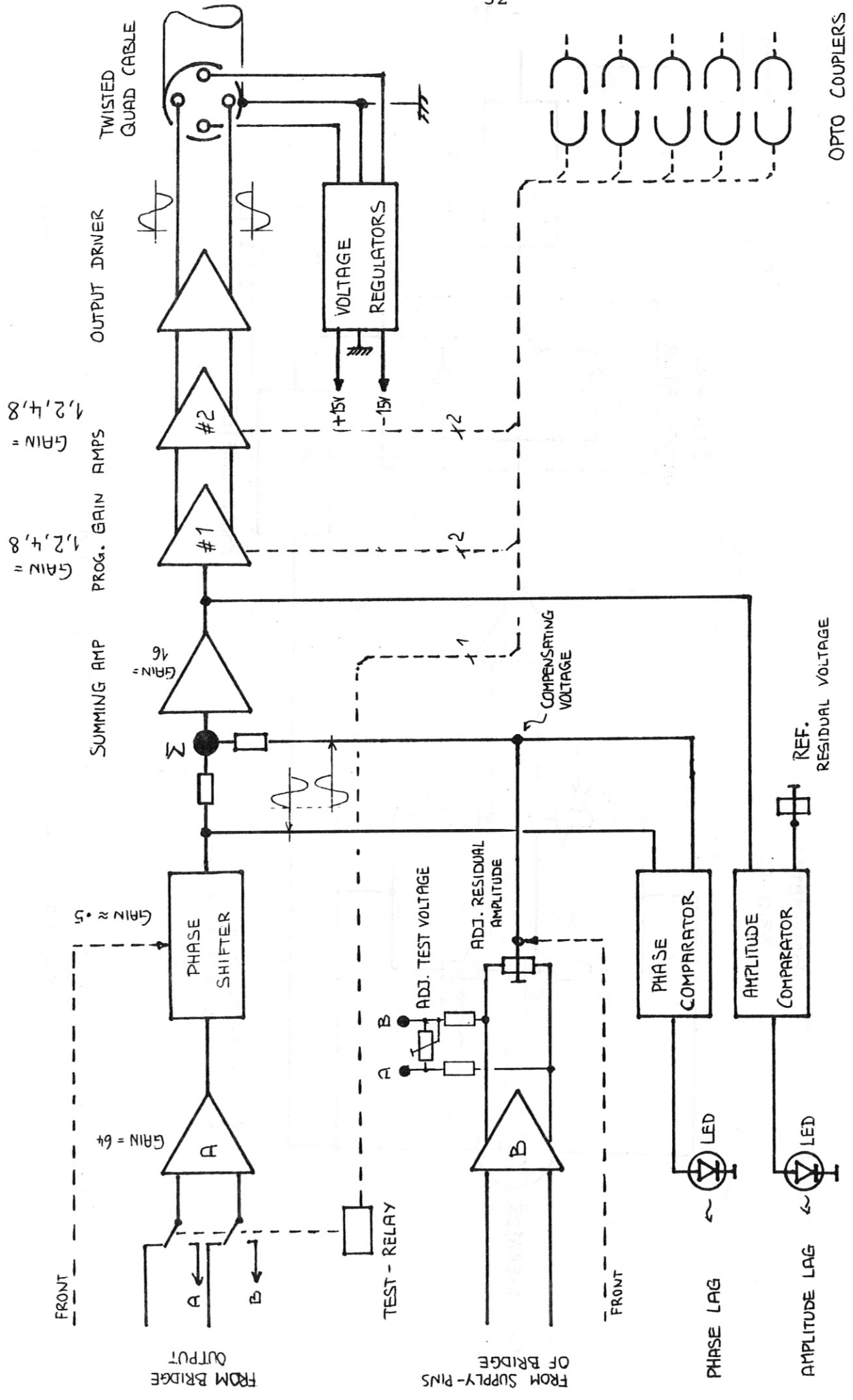


Fig. 13 Block diagram of preamp (for one channel)

11/85 S.S.
IPP

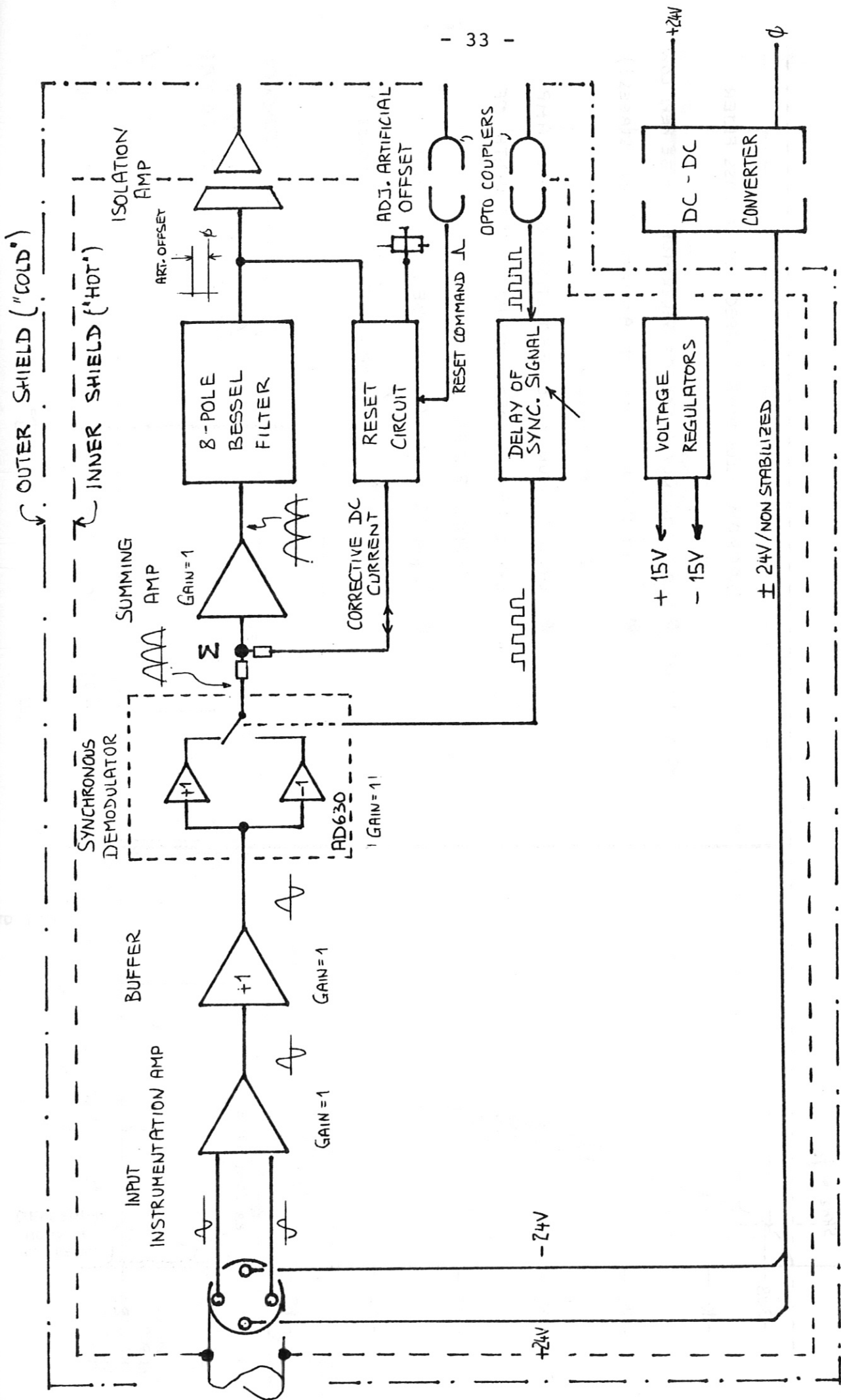


Fig. 14 Block diagram of bolometer "MAIN AMP"

11/85 *SS*
IPF

Fig. 15

Characteristics of low pass filter

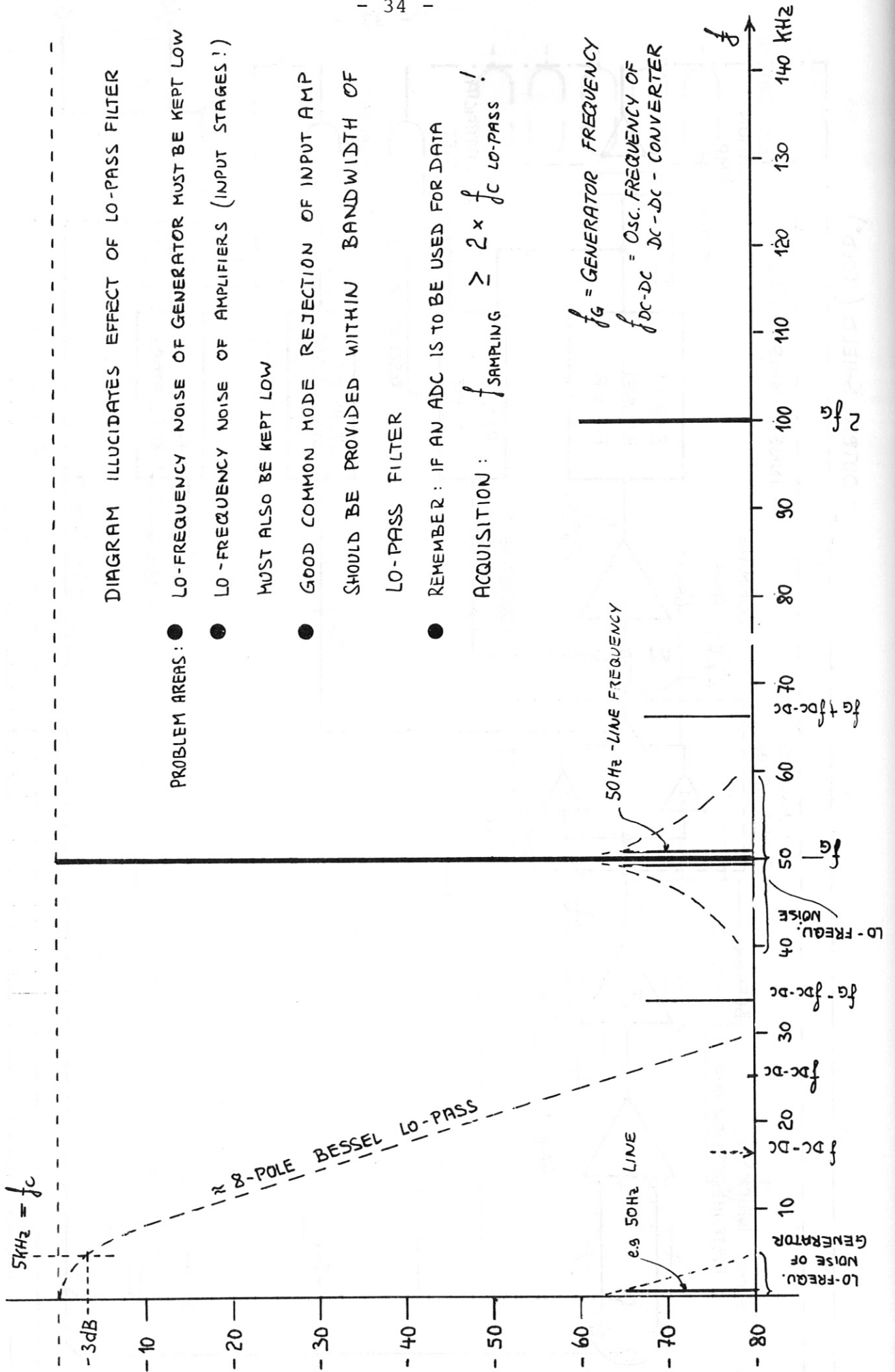


DIAGRAM ILLUSTRATES EFFECT OF LO-PASS FILTER

- PROBLEM AREAS:
- LO-FREQUENCY NOISE OF GENERATOR MUST BE KEPT LOW
 - LO-FREQUENCY NOISE OF AMPLIFIERS (INPUT STAGES!) MUST ALSO BE KEPT LOW
 - GOOD COMMON MODE REJECTION OF INPUT AMP SHOULD BE PROVIDED WITHIN BANDWIDTH OF LO-PASS FILTER
 - REMEMBER: IF AN ADC IS TO BE USED FOR DATA

ACQUISITION: $f_{\text{SAMPLING}} \geq 2 \times f_c$ LO-PASS !

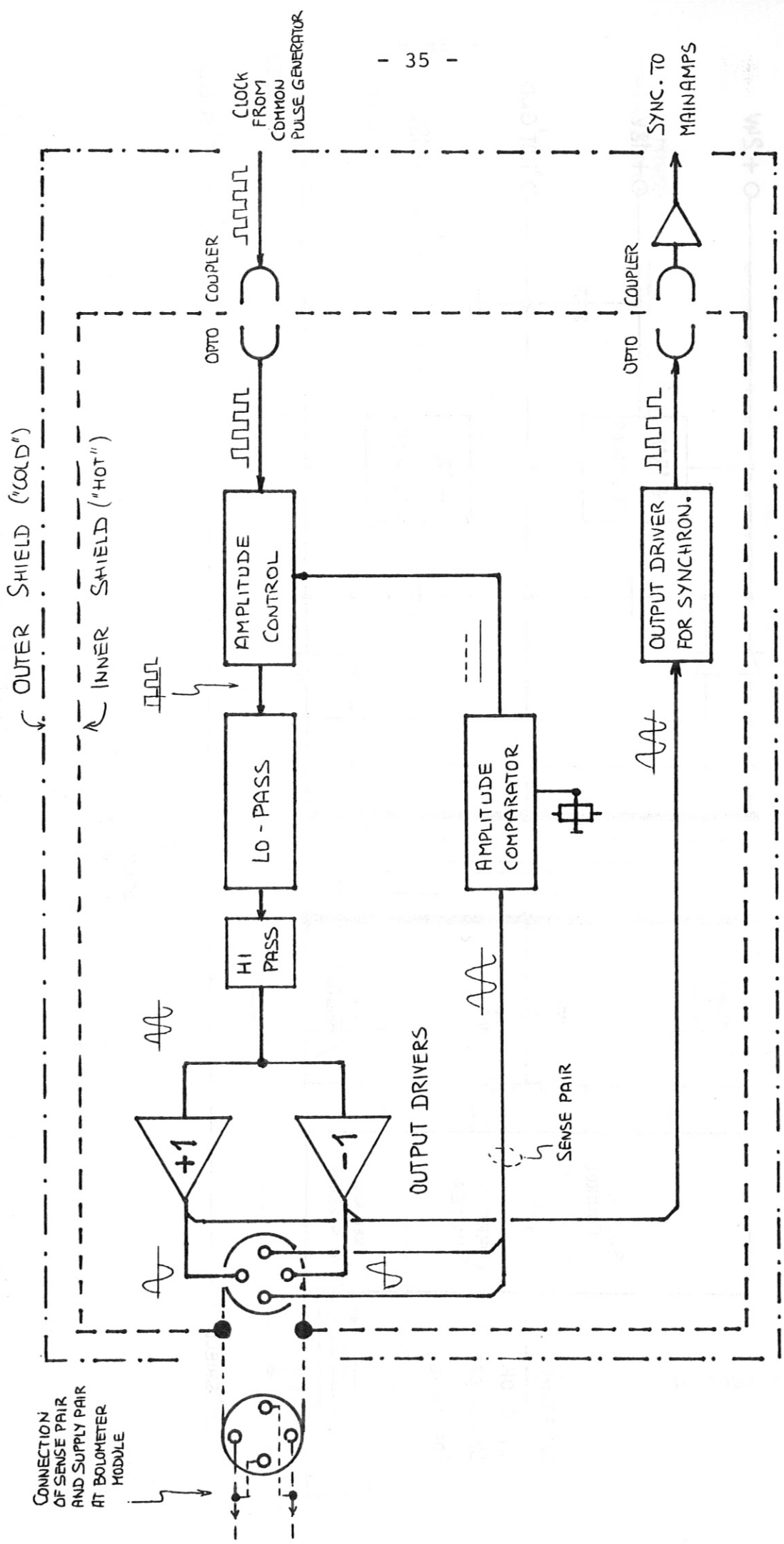


Fig. 16 Block diagram of bridge supply sine generator

11/85 Sch.
IPP

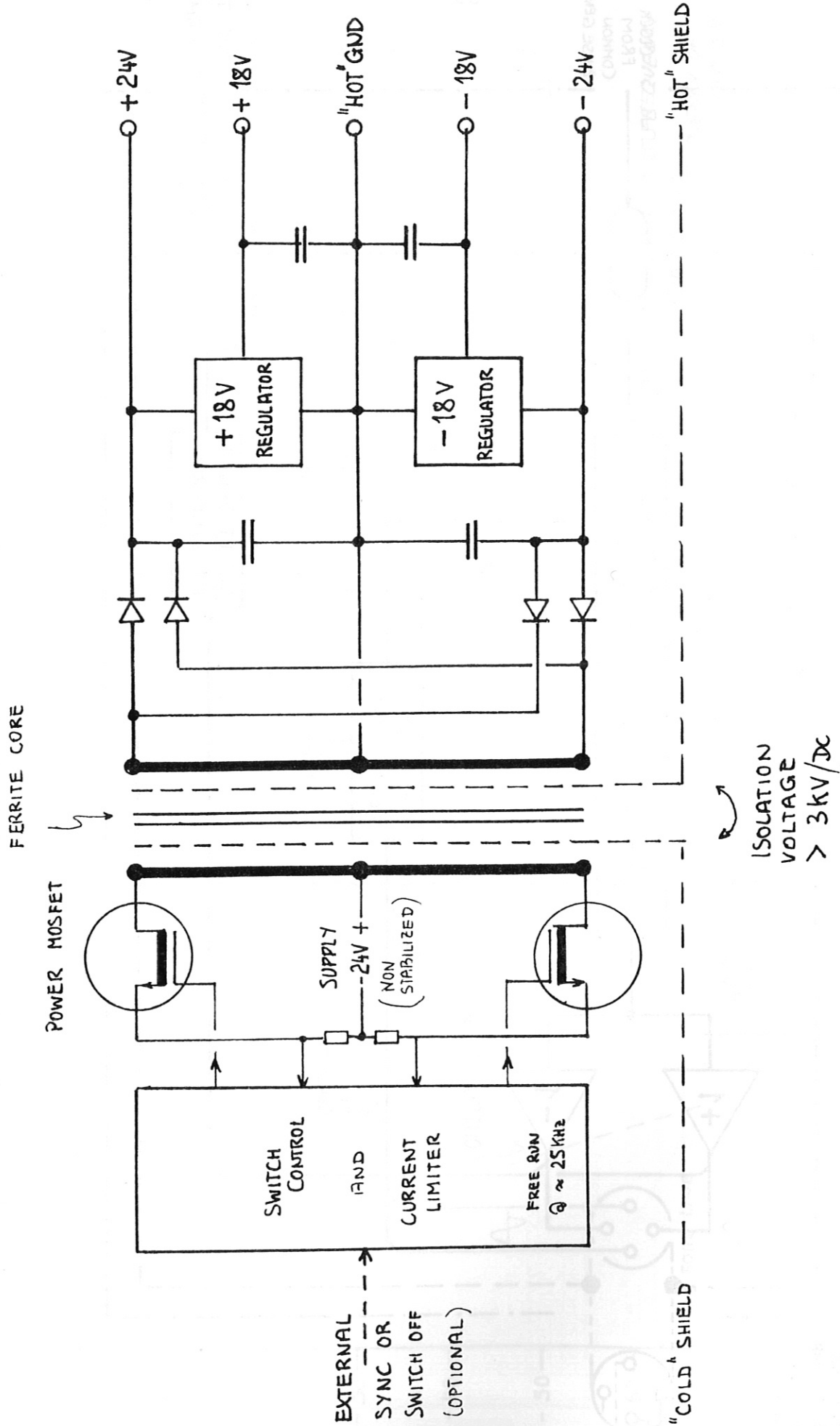
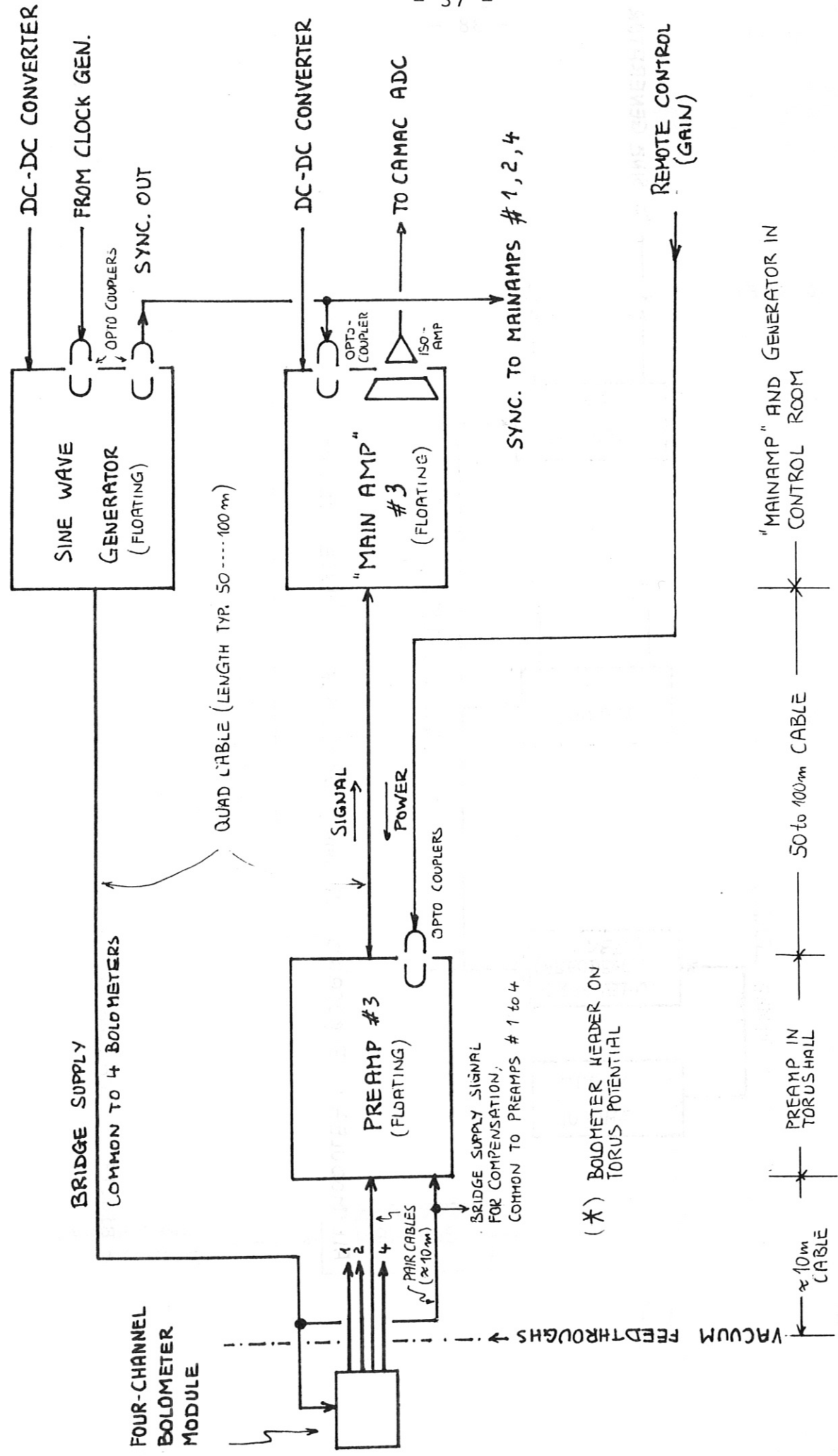


Fig. 17

Simplified circuit diagram of DC-DC converter

11/85 SLo.
IPP



(*) BOLOMETER HEADER ON TORUS POTENTIAL

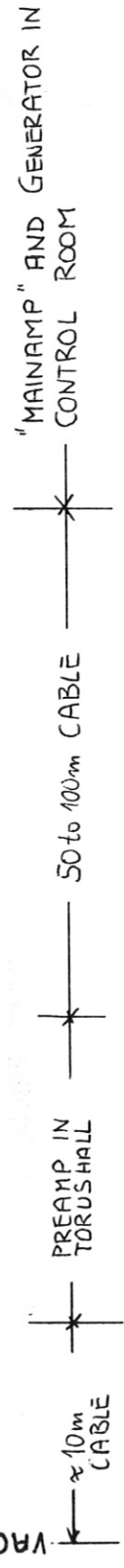
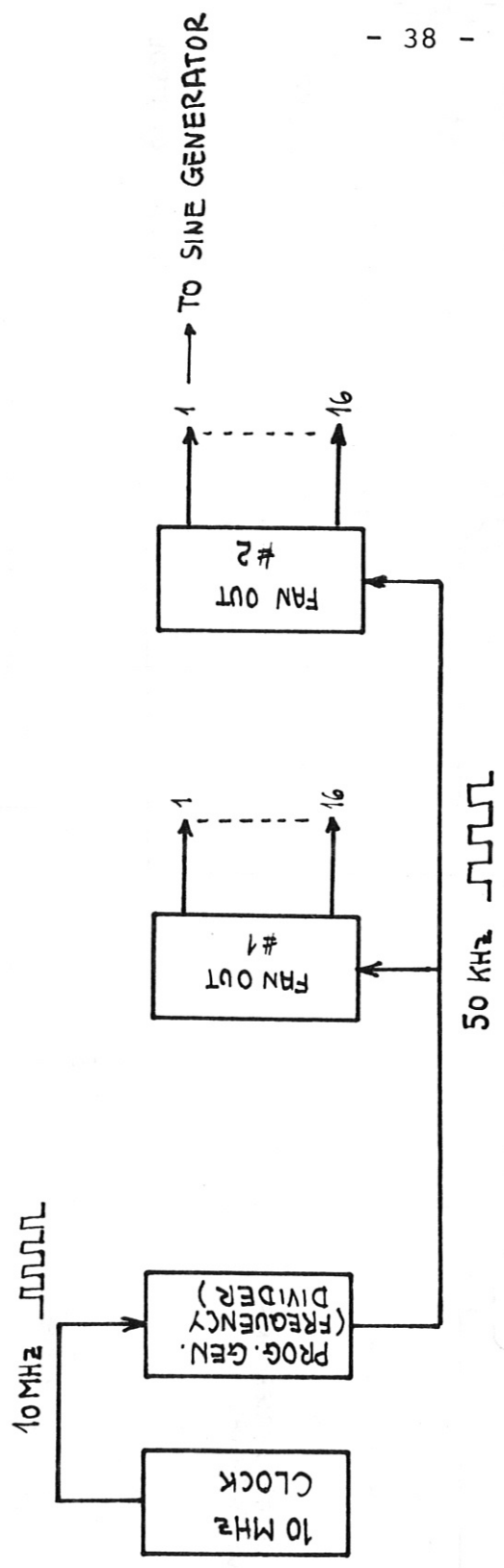


Fig.18 Configuration of bolometer system (only one channel shown)

11/85 SAG
IPF

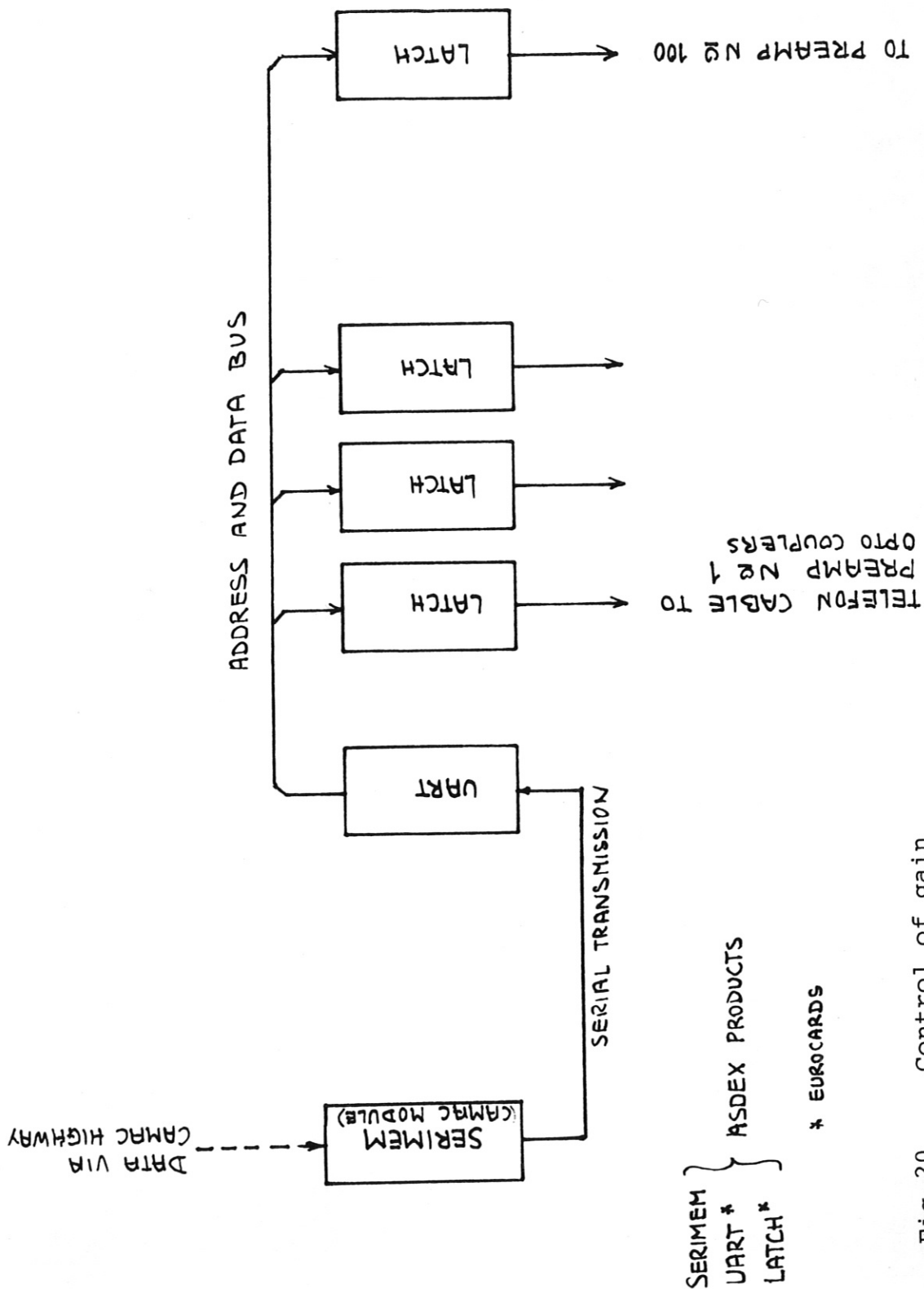


ALL MODULES: EUROCARD 220mm / 6V-SUPPLY } IPP, E1 PRODUCTS

11/85 *SDS*
1PP

Fig.19 Control of sine generators

11/85 S.S.
/PP



SERIMEM }
 UART * } ASDEX PRODUCTS
 LATCH * }
 * EUROCARDS

Fig. 20 Control of gain